

On the Search for Feedback in Reinforcement Learning

Ran Wang¹, Karthikeya S. Parunandi¹, Dan Yu², Dileep Kalathil³, Suman Chakravorty¹

Abstract—This paper addresses the problem of learning the optimal feedback policy for a nonlinear stochastic dynamical system with continuous state space, continuous action space and unknown dynamics. Feedback policies are complex objects that typically need a large dimensional parametrization, which makes Reinforcement Learning algorithms that search for an optimum in this large parameter space, sample inefficient and subject to high variance. We propose a decoupling principle that drastically reduces the feedback parameter space while still remaining near-optimal to the fourth-order in a small noise parameter. Based on this principle, we propose a decoupled data-based control (D2C) algorithm that addresses the stochastic control problem: first, an open-loop deterministic trajectory optimization problem is solved using a black-box simulation model of the dynamical system. Then, a linear closed-loop control is developed around this nominal trajectory using only a simulation model. Empirical evidence suggests significant reduction in training time, as well as the training variance, compared to other state of the art Reinforcement Learning algorithms.

I. INTRODUCTION

Controlling an unknown dynamical system adaptively has a rich history in control literature [1], [2]. This classical literature provides rigorous analysis of the asymptotic performance and stability of the closed loop system. Classical adaptive control literature mainly focuses on non-stochastic systems [3], [4]. Stochastic adaptive control literature mostly addresses tractable models like linear quadratic regulator (LQR) where Riccati equation based closed form expressions are available for the optimal control law. Optimal control of an unknown nonlinear dynamical system with continuous state space and continuous action space is a significantly more challenging problem. Even with a known model, computing an optimal control law requires solving a dynamic programming problem. The ‘curse of dimensionality’ associated with dynamic programming makes solving such problems computationally intractable, except under special structural assumptions on the underlying system. *Learning to control* problems where the model of the system is unknown also suffer from this computational complexity issues, in addition to the usual identifiability problems in adaptive control.

The last few years have seen significant progress in deep neural networks based reinforcement learning approaches for controlling unknown dynamical systems, with applications

in many areas like playing games [5], locomotion [6] and robotic hand manipulation [7]. A number of new algorithms that show promising performance are proposed [8]–[10] and various improvements and innovations have been continuously developed. However, despite excellent performance on many tasks, reinforcement learning (RL) is still considered very data intensive. The training time for such algorithms is typically really large. Moreover, the techniques also suffer from high variance and reproducibility issues [11]. While there have been some attempts to improve the sample efficiency [12], a systematic approach is still lacking.

In this work, we introduce a compact parametrization of feedback policies, consisting of an open loop control sequence and an associated linear feedback policy, that is nonetheless shown to be near-optimal to the true stochastic policy to fourth order, $O(\epsilon^4)$, in a parameter ϵ characterizing the uncertainty in the system. Further, the open loop search is “decoupled” from the feedback search, and thus, leads to a highly efficient search procedure. Based on this result, we propose a novel decoupled data based control (D2C) algorithm for learning to control an unknown nonlinear dynamical system in a completely data based fashion.

Related work: The solution approaches the problem of controlling unknown dynamical systems can be divided into two broad classes, model-based methods and model-free methods.

In the model-based methods, many techniques [13] rely on a discretization of the underlying state and action space, and hence, run into the curse of dimensionality, the fact that the computational complexity grows exponentially with the dimension of the state space of the problem. The most computationally efficient among these techniques are local trajectory-based methods such as differential dynamic programming (DDP) [14], [15] which quadratizes the dynamics and the cost-to-go function around a nominal trajectory. The iterative linear quadratic regulator/ Gaussian (ILQR/ ILQG) [16], [17], which is closely related to DDP, considers the first order expansion of the dynamics (in DDP, a second order expansion is considered), and is shown to be computationally much more efficient. In both approaches, the current linear control policy is executed to compute a new nominal trajectory, and the procedure is repeated until convergence. We note that methods like ILQR/ DDP are open loop search techniques, and thus, can be used within the D2C procedure for the open loop search, if implemented in a model-free fashion. However, we use a simple gradient search technique in this paper and the above algorithmic aspect is left to future work.

Model-free methods, more popularly known as approximate dynamic programming [18], [19] or reinforcement learning

¹R. Wang, K. Parunandi and S. Chakravorty are with the Department of Aerospace Engineering, Texas A&M University, Texas, USA. {rwang0417, s.parunandi, schakrav}@tamu.edu

²D. Yu is with the College of Astronautics, Nanjing University of Aeronautics and Astronautics, Nanjing, 210016, China. yudan@nuaa.edu.cn

³D. Kalathil is with the Department of Electrical and Computer Engineering, Texas A&M University, Texas, USA. dileep.kalathil@tamu.edu

(RL) methods [20], seek to improve the control policy by repeated interactions with the environment while observing the system's responses. The repeated interactions, or learning trials, allow these algorithms to compute the solution of the dynamic programming problem (optimal value/Q-value function or optimal policy) without explicitly constructing the model of the unknown dynamical system. Standard RL algorithms are broadly divided into value-based methods, like Q-learning, and policy-based methods, like policy gradient algorithms. Recently, function approximation using deep neural networks has significantly improved the performance of reinforcement learning algorithms, leading to a growing class of literature on 'deep reinforcement learning'. Despite the success, the number of samples and training time required still seems prohibitive.

Our Contributions are: 1) we show a near optimal parametrization, $O(\epsilon^4)$ with respect to an uncertainty parameter ϵ , of the feedback policy in terms of an open loop control sequence, and a linear feedback control law, 2) we show that the open loop and feedback search can be decoupled, which 3) results in the D2C algorithm that is a highly efficient alternative to state of the art RL techniques, primarily due to the compact feedback parametrization and the decoupled search procedure in the feedback parameter space. *In essence, we advocate an alternative approach to the feedback search at the heart of RL via the "decoupling principle".*

The rest of the paper is organized as follows. In Section II, the basic problem formulation is outlined. In Section III, the main decoupling results which solve the MDP in a 'decoupled open loop-closed loop' fashion are outlined. The proofs of the results are included in the Supplementary document. In Section IV, we propose our decoupled data based control algorithm. In Section V, we test the proposed approach using typical benchmarking examples with comparisons to a state of the art RL technique.

II. PROBLEM FORMULATION

Consider the following discrete time nonlinear stochastic dynamical system:

$$x_{t+1} = h(x_t, u_t, w_t), \quad (1)$$

where $x_t \in \mathbb{R}^{n_x}$, $u_t \in \mathbb{R}^{n_u}$ are the state measurement and control vector at time k , respectively. The process noise w_t is assumed as zero-mean, uncorrelated Gaussian white noise, with covariance W .

The *optimal stochastic control* problem is to find the the control policy $\pi^o = \{\pi_1^o, \pi_2^o, \dots, \pi_{T-1}^o\}$ such that the expected cumulative cost is minimized, i.e.,

$$\begin{aligned} \pi^o &= \arg \min_{\pi} \tilde{J}^{\pi}(x), \quad \text{where,} \\ \tilde{J}^{\pi}(x) &= \mathbb{E}_{\pi} \left[\sum_{t=1}^{T-1} c(x_t, u_t) + c_T(x_T) \mid x_1 = x \right], \quad (2) \end{aligned}$$

$u_t = \pi_t(x_t)$, $c(\cdot, \cdot)$ is the instantaneous cost function, and $c_T(\cdot)$ is the terminal cost function. In the following, we assume that the initial state x_1 is fixed, and denote $\tilde{J}^{\pi}(x)$ simply as \tilde{J}^{π} .

If the function $h(\cdot, \cdot, \cdot)$ is known exactly, then the optimal control law π^o can be computed using dynamic programming method. However, as noted before, this can be often computationally intractable. Moreover, when h is unknown, designing an optimal closed-loop control law is a much more challenging problem. In the following, we propose a data-based decoupled approach for solving (2) when h is unknown.

III. A NEAR OPTIMAL DECOUPLING PRINCIPLE

We first outline a near-optimal decoupling principle in stochastic optimal control that paves the way for the D2C algorithm described in Section IV.

We make the following assumptions for the simplicity of illustration. We assume that the dynamics given in (1) can be written in the form

$$x_{t+1} = f(x_t) + g(x_t)(u_t + \epsilon w_t), \quad (3)$$

where $\epsilon < 1$ is a small parameter. We also assume that the instantaneous cost $c(\cdot, \cdot)$ has the following simple form, $c(x, u) = l(x) + \frac{1}{2}u'Ru$. We emphasize that these assumptions, quadratic control cost and affine in control dynamics, are purely for simplicity of treatment.

A. Characterization of the Performance of Feedback Policies

Consider a noiseless version of the system dynamics given by (3). We denote the "nominal" state trajectory as \bar{x}_t and the "nominal" control as \bar{u}_t where $\bar{u}_t = \pi_t(\bar{x}_t)$, and $\pi = (\pi_t)_{t=1}^{T-1}$ is a given control policy. The resulting dynamics without noise is given by $\bar{x}_{t+1} = f(\bar{x}_t) + g(\bar{x}_t)\bar{u}_t$.

Assuming that $f(\cdot)$, $g(\cdot)$ and $\pi_t(\cdot)$ are sufficiently smooth, we can linearize the dynamics about the nominal trajectory. Denoting $\delta x_t = x_t - \bar{x}_t$, $\delta u_t = u_t - \bar{u}_t$, we can express,

$$\delta x_{t+1} = A_t \delta x_t + B_t \delta u_t + S_t(\delta x_t) + \epsilon w_t, \quad (4)$$

$$\delta u_t = K_t \delta x_t + \tilde{S}_t(\delta x_t), \quad (5)$$

where $A_t = \frac{\partial f}{\partial x} \Big|_{\bar{x}_t} + \frac{\partial g \bar{u}_t}{\partial x} \Big|_{\bar{x}_t}$, $B_t = g(\bar{x}_t)$, $K_t = \frac{\partial \pi_t}{\partial x} \Big|_{\bar{x}_t}$, and $S_t(\cdot)$, $\tilde{S}_t(\cdot)$ are second and higher order terms in the respective expansions. Similarly, we can linearize the instantaneous cost $c(x_t, u_t)$ about the nominal values (\bar{x}_t, \bar{u}_t) as,

$$\begin{aligned} c(x_t, u_t) &= l(\bar{x}_t) + L_t \delta x_t + H_t(\delta x_t) + \\ &\quad \frac{1}{2} \bar{u}_t' R \bar{u}_t + \delta u_t' R \bar{u}_t + \delta u_t' R \delta u_t, \quad (6) \end{aligned}$$

$$c_T(x_T) = c_T(\bar{x}_T) + C_T \delta x_T + H_T(\delta x_T), \quad (7)$$

where $L_t = \frac{\partial l}{\partial x} \Big|_{\bar{x}_t}$, $C_T = \frac{\partial c_T}{\partial x} \Big|_{\bar{x}_T}$, and $H_t(\cdot)$ and $H_T(\cdot)$ are second and higher order terms in the respective expansions.

Using (4) and (5), we can write the closed loop dynamics of the trajectory $(\delta x_t)_{t=1}^T$ as,

$$\delta x_{t+1} = \underbrace{(A_t + B_t K_t)}_{\bar{A}_t} \delta x_t + \underbrace{\{B_t \tilde{S}_t(\delta x_t) + S_t(\delta x_t)\}}_{\tilde{S}_t(\delta x_t)} + \epsilon w_t, \quad (8)$$

where \bar{A}_t represents the linear part of the closed loop systems and the term $\tilde{S}_t(\cdot)$ represents the second and higher order

terms in the closed loop system. Similarly, the closed loop incremental cost given in (6) can be expressed as

$$c(x_t, u_t) = \underbrace{\{l(\bar{x}_t) + \frac{1}{2}\bar{u}_t' R \bar{u}_t\}}_{\bar{c}_t} + \underbrace{[L_t + \bar{u}_t' R K_t]}_{\bar{C}_t} \delta x_t + \underbrace{(K_t \delta x_t + \bar{S}_t(\delta x_t))' R (K_t \delta x_t + \bar{S}_t(\delta x_t))}_{\bar{H}_t(\delta x_t)}. \quad (9)$$

Therefore, the cumulative cost of any given closed loop trajectory $(x_t, u_t)_{t=1}^T$ can be expressed as,

$$\begin{aligned} J^\pi &= \sum_{t=1}^{T-1} c(x_t, u_t = \pi_t(x_t)) + c_T(x_T) \\ &= \sum_{t=1}^T \bar{c}_t + \sum_{t=1}^T \bar{C}_t \delta x_t + \sum_{t=1}^T \bar{H}_t(\delta x_t), \end{aligned} \quad (10)$$

where $\bar{c}_T = c_T(\bar{x}_T)$, $\bar{C}_T = C_T$.

We first show the following critical result.

Lemma 1: Given any sample path, the state perturbation equation $\delta x_{t+1} = \bar{A}_t \delta x_t + \bar{S}_t(\delta x_t) + \epsilon w_t$ given in (8) can be equivalently characterized as $\delta x_t = \delta x_t^l + e_t$, $\delta x_{t+1}^l = \bar{A}_t \delta x_t^l + \epsilon w_t$ where e_t is an $O(\epsilon^2)$ function that depends on the entire noise history $\{w_0, w_1, \dots, w_t\}$ and δx_t^l evolves according to the linear closed loop system. Furthermore, $e_t = e_t^{(2)} + O(\epsilon^3)$, where $e_t^{(2)} = \bar{A}_{t-1} e_{t-1}^{(2)} + \delta x_{t-1}^{l'} \bar{S}_{t-1}^{(2)} \delta x_{t-1}^l$, $e_0^{(2)} = 0$, and $\bar{S}_t^{(2)}$ represents the Hessian corresponding to the Taylor series expansion of the function $\bar{S}_t(\cdot)$.

Next, we have the following result for the expansion of the cost to go function J^π .

Lemma 2: Given any sample path, the cost-to-go under a policy can be expanded as: $J^\pi = \underbrace{\sum_t \bar{c}_t}_{\bar{J}^\pi} + \underbrace{\sum_t \bar{C}_t \delta x_t^l}_{\delta J_1^\pi} + \underbrace{\sum_t \delta x_t^{l'} \bar{H}_t^{(2)} \delta x_t^l + \bar{C}_t e_t^{(2)}}_{\delta J_2^\pi} + O(\epsilon^3)$,

where $\bar{H}_t^{(2)}$ denotes the second order coefficient of the Taylor expansion of $\bar{H}_t(\cdot)$.

Now, we show the following important result.

Proposition 1:

$$\begin{aligned} \tilde{J}^\pi &= \mathbb{E}[J^\pi] = \bar{J}^\pi + O(\epsilon^2), \\ \text{Var}(J^\pi) &= \underbrace{\text{Var}(\delta J_1^\pi)}_{O(\epsilon^2)} + O(\epsilon^4). \end{aligned}$$

All proofs can be found in the supplementary file.

A further consequence of the result above is the following. Suppose that given a policy $\pi_t(\cdot)$, we only consider the linear part, i.e., the linear approximation $\pi_t^l(x_t) = \bar{u}_t + K_t \delta x_t$. According to Lemmas 1 and 2, the $O(\epsilon^2)$ terms in the expansion of the cost of any sample path solely result from the linear closed loop system. Therefore, it follows that the sample path cost under the full policy $\pi_t(\cdot)$ and the linear policy $\pi_t^l(\cdot)$ agree up to the ϵ^2 term. Therefore, it follows that $|E[J^\pi] - E[J^{\pi^l}]| = O(\epsilon^4)$. We summarize this result in the following result:

Proposition 2: Let $\pi_t(\cdot)$ be any given feedback policy. Let $\pi_t^l(x_t) = \bar{u}_t + K_t \delta x_t$ be the linear approximation of the

policy. Then, the error in the expected cost to go under the two policies, $|E[J^\pi] - E[J^{\pi^l}]| = O(\epsilon^4)$.

Propositions 1 and 2 form the basis of an $O(\epsilon^2)$ and an $O(\epsilon^4)$ decoupling result in the following subsections.

B. An $O(\epsilon^2)$ Near-Optimal Decoupled Approach for Closed Loop Control

Proposition 1 suggests that an open loop control super imposed with a closed loop control for the perturbed linear system may be approximately optimal. We delineate this idea below.

Open Loop Design. First, we design an optimal (open loop) control sequence \bar{u}_t^* for the noiseless system. More precisely,

$$\begin{aligned} (\bar{u}_t^*)_{t=1}^{T-1} &= \arg \min_{(\bar{u}_t)_{t=1}^{T-1}} \sum_{t=1}^{T-1} c(\bar{x}_t, \bar{u}_t) + c_T(\bar{x}_T), \quad (11) \\ \bar{x}_{t+1} &= f(\bar{x}_t) + g(\bar{x}_t) \bar{u}_t. \end{aligned}$$

We will discuss the details of this open loop design in Section IV.

Closed Loop Design. We find the optimal feedback gain K_t^* such that the variance of the linear closed loop system around the nominal path, (\bar{x}_t, \bar{u}_t^*) , from the open loop design above, is minimized.

$$\begin{aligned} (K_t^*)_{t=1}^{T-1} &= \arg \min_{(K_t)_{t=1}^{T-1}} \text{Var}(\delta J_1^\pi), \\ \delta J_1^\pi &= \sum_{t=1}^T \bar{C}_t \delta x_t^l, \\ \delta x_{t+1}^l &= (A_t + B_t K_t) \delta x_t^l + \epsilon w_t. \end{aligned} \quad (12)$$

We now characterize the approximate closed loop policy below.

Proposition 3: Construct a closed loop policy $\pi_t^*(x_t) = \bar{u}_t^* + K_t^* \delta x_t$, where \bar{u}_t^* is the solution of the open loop problem (11), and K_t^* is the solution of the closed loop problem (12). Let π^o be the optimal closed loop policy. Then, $|\tilde{J}^{\pi^o} - \tilde{J}^{\pi^*}| = O(\epsilon^2)$. Furthermore, among all policies with nominal control action \bar{u}_t^* , the variance of the cost-to-go under policy π_t^* , is within $O(\epsilon^4)$ of the variance of the policy with the minimum variance.

Unfortunately, there is no standard solution to the closed-loop problem (12) due to the non additive nature of the cost function $\text{Var}(\delta J_1^\pi)$. Therefore, we solve a standard LQR problem as a surrogate, and the effect is again one of reducing the variance of the cost-to-go by reducing the variance of the closed-loop trajectories.

Approximate Closed Loop Problem. We solve the following LQR problem for suitably defined cost function weighting factors Q_t, R_t :

$$\begin{aligned} \min_{(\delta u_t)_{t=1}^T} & \mathbb{E} \left[\sum_{t=1}^{T-1} \delta x_t' Q_t \delta x_t + \delta u_t' R_t \delta u_t + \delta x_T' Q_T \delta x_T \right], \\ \delta x_{t+1} &= A_t \delta x_t + B_t \delta u_t + \epsilon w_t. \end{aligned} \quad (13)$$

The solution to the above problem furnishes us a feedback gain \hat{K}_t^* which we can use in the place of the true variance minimizing gain K_t^* .

C. An $O(\epsilon^4)$ Near-Optimal Decoupled Approach for Closed Loop Control

In order to derive the results in this section, we need some additional structure on the dynamics. *In essence, the results in this section require that the time discretization of the dynamics be small enough.* Thus, let the dynamics be given by:

$$x_t = x_{t-1} + \bar{f}(x_{t-1})\Delta t + \bar{g}(x_{t-1})u_t\Delta t + \epsilon\omega_t\sqrt{\Delta t}, \quad (14)$$

where ω_t is a white noise sequence, and the sampling time Δt is small enough that $O(\Delta t^\alpha)$ is negligible for $\alpha > 1$. The noise term above is a Brownian motion, and hence the $\sqrt{\Delta t}$ factor. Further, the incremental cost function $c(x, u)$ is given as: $c(x, u) = \bar{l}(x)\Delta t + \frac{1}{2}u'\bar{R}u\Delta t$. The main reason to use the above assumptions is to simplify the Dynamic Programming (DP) equation governing the optimal cost-to-go function of the system. The DP equation for the above system is given by:

$$J_t(x) = \min_{u_t} \{c(x, u) + E[J_{t+1}(x')]\}, \quad (15)$$

where $x' = x + \bar{f}(x)\Delta t + \bar{g}(x)u_t\Delta t + \epsilon\omega_t\sqrt{\Delta t}$ and $J_t(x)$ denotes the cost-to-go of the system given that it is at state x at time t . The above equation is marched back in time with terminal condition $J_T(x) = c_T(x)$, and $c_T(\cdot)$ is the terminal cost function. Let $u_t(\cdot)$ denote the corresponding optimal policy. Further, let $u_t^d(\cdot)$ be the optimal control policy for the deterministic system, i.e., Eq. 14 with $\epsilon = 0$. Next, let $\varphi_t(\cdot)$ denote the cost-to-go of the deterministic policy when applied to the stochastic system, i.e., u_t^d applied to Eq. 29 with $\epsilon > 0$. Then, we have the following important result.

Proposition 4: The difference between the cost function of the optimal stochastic policy, J_t , and the cost function of the “deterministic policy applied to the stochastic system”, φ_t , is $O(\epsilon^4)$, i.e. $|J_t(x) - \varphi_t(x)| = O(\epsilon^4)$ for all (t, x) . The above result was originally proved in a seminal paper [21] for continuous time, first passage problems. We have provided a simple derivation of the result, in the context of a discrete time finite horizon problem, in the Supplementary document.

Given some initial condition x_0 , consider a linear truncation of the optimal deterministic policy, i.e., let $u_t^l(\cdot) = \bar{u}_t + K_t\delta x_t$, where the deterministic policy is given by $u_t^d = \bar{u}_t + K_t\delta x_t + S_t(\delta x_t)$, where $S_t(\cdot)$ denote the second and higher order terms in the optimal deterministic feedback policy. Using Proposition 2, it follows that the cost of the linear policy, say $\varphi_t^l(\cdot)$, is within $O(\epsilon^4)$ of the cost of the deterministic policy $u_t^d(\cdot)$, when applied to the stochastic system in Eq. 14. However, the result in Proposition 4 shows that the cost of the deterministic policy is within $O(\epsilon^4)$ of the optimal stochastic policy. Taken together, this implies that the cost of the linear deterministic policy is within $O(\epsilon^4)$ of the optimal stochastic policy. This may be summarized in the following result.

Proposition 5: Let the optimal cost function under the true stochastic policy be given $J_t(\cdot)$. Let the optimal deterministic

policy be given by $u_t^d(x_t) = \bar{u}_t + K_t\delta x_t + S_t(\delta x_t)$, and the linear approximation to the policy be $u_t^l(x_t) = \bar{u}_t + K_t\delta x_t$, and let the cost of the linear policy be given by $\varphi_t^l(x)$. Then $|J_t(x) - \varphi_t^l(x)| = O(\epsilon^4)$ for all (t, x) .

Now, it remains to be seen how to design the \bar{u}_t and the linear feedback term K_t . The open loop optimal control sequence \bar{u}_t is found identically to the previous section. However, the linear feedback gain K_t is calculated in a slightly different fashion and may be done as shown in the following result. In the following, $\mathcal{F}(x) = x + \bar{f}(x)\Delta t$, $\mathcal{G}(x) = \bar{g}(x)\Delta t$, $A_t = \frac{\partial \mathcal{F}}{\partial x}|_{\bar{x}_t} + \frac{\partial \mathcal{G}}{\partial x}\bar{u}_t|_{\bar{x}_t}$, $B_t = \mathcal{G}(\bar{x}_t)$, $L_t = \frac{\partial l}{\partial x}|_{\bar{x}_t}$ and $L_{tt} = \nabla_{xx}^2 l|_{\bar{x}_t}$. Let $\phi_t(x_t)$ denote the optimal cost-to-go of the deterministic problem, i.e., Eq 14 with $\epsilon = 0$.

Proposition 6: Decoupled Design. Given an optimal nominal trajectory (\bar{x}_t, \bar{u}_t) , the backward evolutions of the first and second derivatives, $G_t = \frac{\partial \phi_t}{\partial x}|_{\bar{x}_t}$ and $P_t = \nabla_{xx}^2 \phi_t|_{\bar{x}_t}$, of the optimal cost-to-go function $\phi_t(x_t)$, initiated with the terminal boundary conditions $G_N = \frac{\partial c_N(x_N)}{\partial x_N}|_{\bar{x}_N}$ and $P_N = \nabla_{xx}^2 c_N|_{\bar{x}_N}$ respectively, are as follows:

$$G_t = L_t + G_{t+1}A_t \quad (16)$$

$$P_t = L_{tt} + A_t'P_{t+1}A_t - K_t'S_tK_t + G_{t+1} \otimes \tilde{R}_{t,xx} \quad (17)$$

for $t = \{0, 1, \dots, N-1\}$, where, $S_t = (R_t + B_t'P_{t+1}B_t)$, $K_t = -S_t^{-1}(B_t'P_{t+1}A_t + (G_{t+1} \otimes \tilde{R}_{t,xx})')$, $\tilde{R}_{t,xx} = \nabla_{xx}^2 \mathcal{F}(x_t)|_{\bar{x}_t} + \nabla_{xx}^2 \mathcal{G}(x_t)|_{\bar{x}_t, \bar{u}_t}$, $\tilde{R}_{t,xx} = \nabla_{xu}^2 (\mathcal{F}(x_t) + \mathcal{G}(x_t)u_t)|_{\bar{x}_t, \bar{u}_t}$ where ∇_{xx}^2 represents the Hessian of a vector-valued function w.r.t x and \otimes denotes the tensor product.

Summary of the Decoupling Results and Implications

The previous two subsections showed that the feedback parameterization can be written as: $\pi_t(x_t) = \bar{u}_t + K_t\delta x_t$, where $\delta x_t = x_t - \bar{x}_t$ denotes the state deviation from the nominal. Further, it was shown that the optimal open loop sequence \bar{u}_t is independent of the feedback gain, while the feedback gain K_t can be designed based on the optimal \bar{u}_t . Hence, the term *decoupling*, in the sense that the search for the optimal parameter (\bar{u}_t^*, K_t^*) need not be done jointly. Moreover, it was shown that depending on how one designed the gain K_t , we can obtain either $O(\epsilon^2)$ (Proposition 3), or $O(\epsilon^4)$ (Propositions 6), near-optimality to the true stochastic policy.

IV. DECOUPLED DATA BASED CONTROL (D2C) ALGORITHM

In this section, we proposed a novel decoupled data-based control (D2C) algorithm formalizing the ideas proposed in Section III. First, a noiseless open-loop optimization problem is solved to find a nominal optimal trajectory. Then a linearized closed-loop controller is designed around this nominal trajectory, such that, with the existence of stochastic perturbations, the state stays close to the optimal open-loop

trajectory. In the following section, we discuss each of the above steps.

A. Open Loop Trajectory Optimization

A first-order gradient descent method is used here for the open-loop optimization problem given in (11), where the underlying dynamic model is used as a blackbox, and the necessary gradients are found from a sequence of input perturbation experiment data using standard least square.

Denote the initial guess of the control sequence as $U^{(0)} = \{\bar{u}_t^{(0)}\}_{t=0}^{T-1}$, and the corresponding states $\mathcal{X}^{(0)} = \{\bar{x}_t^{(0)}\}_{t=0}^T$. The control policy is updated iteratively via $U^{(n+1)} = U^{(n)} - \alpha \nabla_U \bar{J}|_{\mathcal{X}^{(n)}, U^{(n)}}$, where $U^{(n)} = \{\bar{u}_t^{(n)}\}_{t=0}^{T-1}$ denotes the control sequence in the n^{th} iteration, $\mathcal{X}^{(n)} = \{\bar{x}_t^{(n)}\}_{t=0}^T$ denotes the corresponding states, and α is the step size parameter. As $\bar{J}|_{\mathcal{X}^{(n)}, U^{(n)}}$ is the expected cumulative cost under control sequence $U^{(n)}$ and corresponding states $\mathcal{X}^{(n)}$, the gradient vector is defined as $\nabla_U \bar{J}|_{\mathcal{X}^{(n)}, U^{(n)}} = \left(\frac{\partial \bar{J}}{\partial u_1} \quad \frac{\partial \bar{J}}{\partial u_1} \quad \cdots \quad \frac{\partial \bar{J}}{\partial u_T} \right) |_{\mathcal{X}^{(n)}, U^{(n)}}$, which is the gradient of the expected cumulative cost w.r.t the control sequence after n iterations. The following paragraph elaborates on how to estimate the above gradient.

Let us define a rollout to be an episode in the simulation that starts from the initial settings to the end of the horizon with a control sequence. For each iteration, multiple rollouts are conducted sequentially with both the expected cumulative cost and the gradient vector updated iteratively after each rollout. During one iteration for the control sequence, the expected cumulative cost is calculated as $\bar{J}|_{\mathcal{X}^{(n)}, U^{(n)}}^{j+1} = (1 - \frac{1}{j}) \bar{J}|_{\mathcal{X}^{(n)}, U^{(n)}}^j + \frac{1}{j} (J|_{\mathcal{X}^{j,(n)}, U^{j,(n)}})$, where j denotes the j^{th} rollout within the current iteration process of control sequence. $\bar{J}|_{\mathcal{X}^{(n)}, U^{(n)}}^j$ is the expected cumulative cost after j rollouts while $J|_{\mathcal{X}^{j,(n)}, U^{j,(n)}}$ denotes the cost of the j^{th} rollout under control sequence $U^{j,(n)}$ and corresponding states $\mathcal{X}^{j,(n)}$. Note that $U^{j,(n)} = \{\bar{u}_t^{(n)} + \delta u_t^{j,(n)}\}_{t=0}^{T-1}$ where $\{\delta u_t^{j,(n)}\}_{t=0}^{T-1}$ is the zero-mean, i.i.d Gaussian noise added as perturbation to the control sequence $U^{(n)}$.

Then the gradient vector is calculated in a similar sequential manner as $\nabla_U \bar{J}|_{\mathcal{X}^{(n)}, U^{(n)}}^{j+1} = (1 - \frac{1}{j}) \nabla_U \bar{J}|_{\mathcal{X}^{(n)}, U^{(n)}}^j + \frac{1}{j \sigma_{\delta u}} (J|_{\mathcal{X}^{j,(n)}, U^{j,(n)}} - \bar{J}|_{\mathcal{X}^{(n)}, U^{(n)}}^{j+1}) (U^{j,(n)} - U^{(n)})$, where $\sigma_{\delta u}$ is the variance of the control perturbation and $\nabla_U \bar{J}|_{\mathcal{X}^{(n)}, U^{(n)}}^{j+1}$ denotes the gradient vector after j rollouts. Note that after each rollout, both the expected cumulative cost and the gradient vector are updated. The rollout number m in one iteration for the control sequence is decided by the convergence of both the expected cumulative cost and the gradient vector. After m rollouts, the control sequence is updated using the gradient descent equation above in which $\nabla_U \bar{J}|_{\mathcal{X}^{(n)}, U^{(n)}}$ is estimated by $\nabla_U \bar{J}|_{\mathcal{X}^{(n)}, U^{(n)}}^m$. We repeat this until the cost converges and the optimized nominal control sequence is $\{\bar{u}_t^*\}_{t=0}^{T-1} = \{\bar{u}_t^{(N)}\}_{t=0}^{T-1}$.

B. Linear Time-Varying System Identification

Closed loop control design specified in (12) or the approximate closed loop control design specified in (13)

requires the knowledge of the parameters $A_t, B_t, 0 \leq t < T$, of the perturbed linear system. We propose a linear time variant (LTV) system identification procedure to estimate these parameters.

First start from perturbed linear system given by equation (13). Using only first order information and estimate the system parameters A_t, B_t with the following form $\delta x_{t+1} = \hat{A}_t \delta x_t + \hat{B}_t \delta u_t$, rewrite with augmented matrix $\delta x_{t+1} = [\hat{A}_t \mid \hat{B}_t] \begin{bmatrix} \delta x_t \\ \delta u_t \end{bmatrix}$, Now write out their components for each iteration in vector form as, $Y = [\delta x_{t+1}^0 \delta x_{t+1}^1 \cdots \delta x_{t+1}^{N-1}]$, $X = \begin{bmatrix} \delta x_t^0 & \delta x_t^1 & \cdots & \delta x_t^{N-1} \\ \delta u_t^0 & \delta u_t^1 & \cdots & \delta u_t^{N-1} \end{bmatrix}$, $Y = [\hat{A}_t \mid \hat{B}_t] X$, where N is the total iteration number. δx_{t+1}^n denotes the output state deviation, δx_t^n denotes the input state perturbations and δu_t^n denotes the input control perturbations at time t of the n^{th} iteration. All the perturbations are zero-mean, i.i.d, Gaussian random vectors whose covariance matrix is σI where I is the identity matrix and σ is a scalar. Using the least square method, \hat{A}_t and \hat{B}_t can then be calculated as: $[\hat{A}_t \mid \hat{B}_t] = \frac{1}{\sigma N} Y X'$.

Given the estimated perturbed linear system, we design a finite horizon, discrete time LQR [22] along the trajectory for each time step.

Algorithm 1: D2C Algorithm

- 1) Solve the deterministic open-loop optimization problem for optimal open loop nominal control sequence and trajectory $(\{\bar{u}_t^*\}_{t=0}^{T-1}, \{\bar{x}_t^*\}_{t=0}^T)$ using gradient descent method (Section IV-A).
 - 2) Identify the LTV system (\hat{A}_t, \hat{B}_t) via least square estimation (Section IV-B).
 - 3) Solve the Riccati equations using estimated LTV system equation for feedback gain $\{K_t\}_{t=0}^{T-1}$.
 - 4) Set $t = 0$, given initial state $x_0 = \bar{x}_0^*$ and state deviation $\delta x_0 = 0$.
- while** $t < T$ **do**
- $$u_t = \bar{u}_t^* + K_t \delta x_t,$$

$$x_{t+1} = f(x_t) + B_t(u_t + \epsilon w_t),$$

$$\delta x_{t+1} = x_{t+1} - \bar{x}_{t+1}^* \tag{18}$$
- $t = t + 1.$
- end while**
-

The Decoupled Data Based Control (D2C) Algorithm is summarized in Algorithm 1.

V. EMPIRICAL RESULTS

In this section, we compare the D2C approach with the well-known deep reinforcement learning algorithm - Deep Deterministic Policy Gradient (DDPG) [23]. For the comparison, we evaluate both the methods in the following three aspects:

Efficiency in training - the amount of time and storage required to achieve the desired task.

Robustness to noise- the deviation from the predefined task due to random noise in process in the testing stage.

Ease of training - the challenges involved in training with either of the data-based approaches.

More details regarding the experiments presented here, as well as other related experiments, can be found in the supplementary document.

A. Tasks and Implementation

We tested our method with five benchmark tasks, all implemented in MuJoCo simulator [24]: Inverted pendulum, Cart-pole, 3-link swimmer, 6-link swimmer and fish [25]. The systems, which range from 2 to 26 in state dimensions, and 1 to 6 control inputs, and their tasks, are defined in the supplementary document.

D2C implementation is done as outlined in the previous section and ‘MuJoCo Pro 150’ is used as the environment for simulating the blackbox model. An off-the-shelf implementation of DDPG provided by *Keras-RL* [26] library has been customized for our simulations. For comparison, ‘Episodic reward/cost fraction’ is considered with both methods. It is defined as the fraction of reward obtained in an episode during training w.r.t the nominal episodic reward (converged reward). Note that the words ‘reward’ and ‘cost’ are being used interchangeably due to their different notions in optimal control and RL literature respectively, though they achieve the same objective. For simplicity, one is considered the negative of the other. Five hundred Monte-Carlo runs were operated in the testing part. All experiments were run on a personal laptop with I7-7700HQ CPU.

B. Performance Comparison

Training-efficiency: One way of measuring efficient training is to collate the times taken for the episodic cost (or reward) to converge during training. Plots in Fig. 1 show the training process with both methods on the systems considered. Table II delineates the times taken for training respectively. As the system identification and feedback gain calculation in case of D2C take only a small fraction of the time, the total time comparison in Table II shows that D2C learns the optimal policy substantially faster than DDPG and hence, has significantly better efficiency. In our opinion, the primary reason for this disparity is the feedback parametrization of the two methods, the size of the DDPG deep neural nets is significantly larger than the D2C open loop sequence (Table I), and given that both methods use gradient descent, it is not surprising that D2C takes much less time.

Robustness to noise: As with canonical off-policy RL algorithms, DDPG requires that an exploration noise should be added to the policy, during training. Given that the training adapts the policy to various levels of noise, combined with hours of intense training and a nonlinear policy output, it may be expected that it is more robust towards noise as seems evident from Figs. 2 (c) and 2 (d). However, from plots in Figs. 2 (a),(b) and (d), it is evident that in some systems, the performance of D2C is at least on par with or better than DDPG. However, we also note that by the time the DDPG

TABLE I: Parameter size comparison between D2C and DDPG

System	No. of steps	No. of actuators	No. of parameters optimized in D2C	No. of parameters optimized in DDPG
Inverted Pendulum	30	1	30	244002
Cart pole	30	1	30	245602
3-link Swimmer	1600	2	3200	251103
6-link Swimmer	1500	5	7500	258006
Fish	1200	6	7200	266806

performance becomes better, the actual performance of both methods has deteriorated to unacceptable levels. It may also be noted that the error variance in the D2C method increases when the noise level is higher than a threshold and drives the system too far away from the nominal trajectory that the LQR controller cannot fix it. This could be considered a drawback for D2C. However, it must be noted that the range of noise levels (up until 100 % of the maximum control signal) that we are considering here is far beyond what is typically encountered in practical scenarios. Hence, the performance of D2C can be seen to be satisfactory for reasonable amounts of noise in the system.

Ease of training: By this, we mean the challenges associated with implementation. Reproducibility [11] is still a major challenge that RL is yet to overcome. On the other hand, training in D2C is predictable and has low variance. To elucidate the ease of training from an empirical perspective, the exploration noise that is required for training in DDPG mandates the system to operate with a shorter time-step than a threshold, beyond which the simulation fails due to an excessive level of control. To show this, we train both the 3 and 6 link swimmers in one such case (with $\Delta t = 0.01$ sec) until it fails and execute the intermediate policy. Fig. 3 shows the plot in the testing-stage with both methods. It is evident from the terminal state mean-squared error at zero noise level that the nominal trajectory of DDPG is incomplete and its policy failed to reach the goal. The effect is more pronounced in the higher-dimensional 6-link swimmer system (Fig. 3b). On the other hand, the D2C training results in a working policy in a reliable fashion. The same effect is seen in the fish example in Fig. 2(d).

VI. CONCLUSIONS

In this paper, we have proposed a near-optimal decoupling principle for stochastic control resulting in the D2C algorithm. We tested its performance and juxtaposed them with a state-of-the-art deep RL technique - DDPG. From the results, our method has a significant advantage over DDPG in training efficiency, while not sacrificing unduly on performance, primarily due to the compact parametrization of the feedback search.

We hope that our approach signifies the potential of

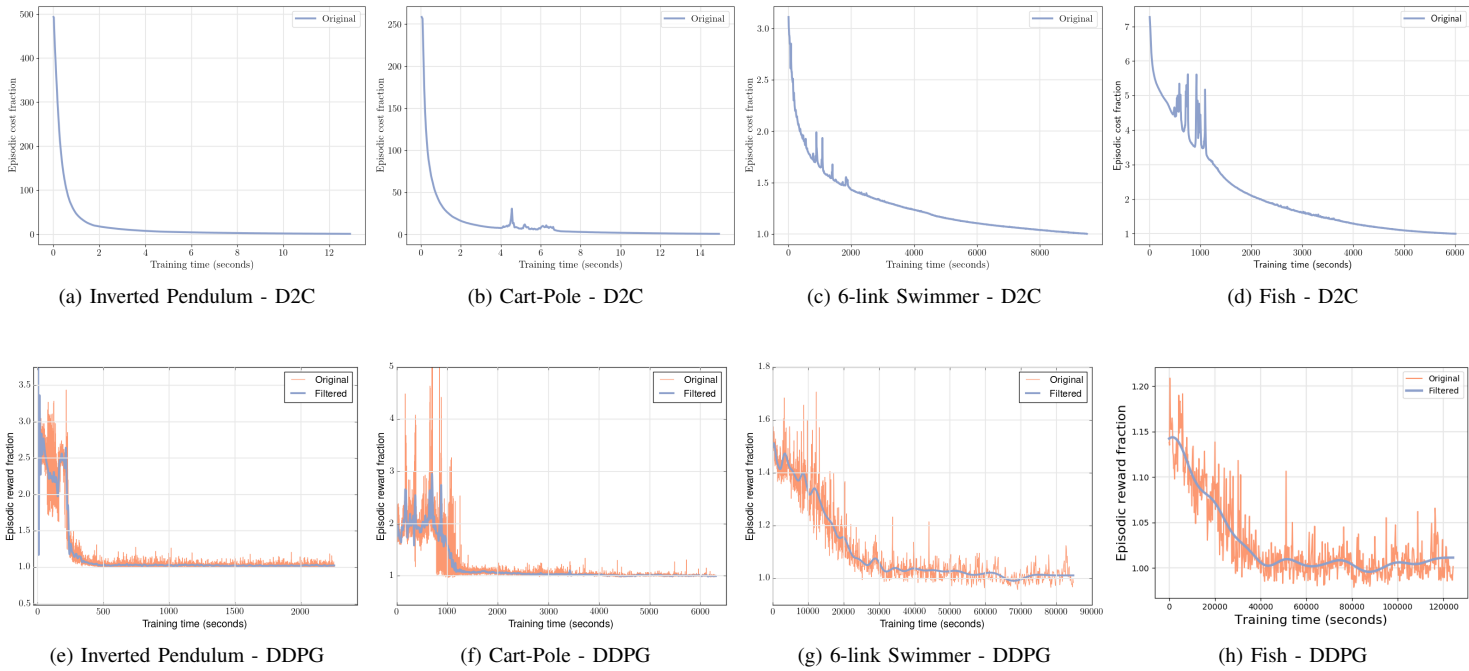


Fig. 1: Episodic cost fraction vs time taken during training

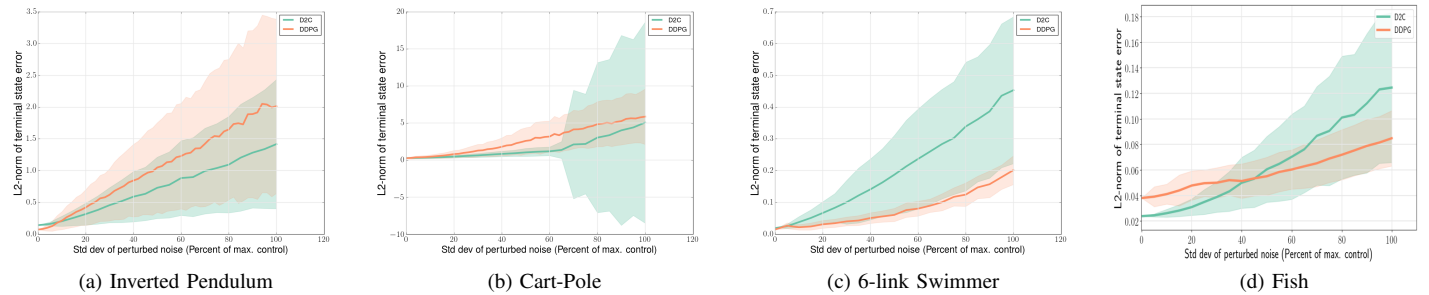


Fig. 2: Terminal MSE vs noise level during testing

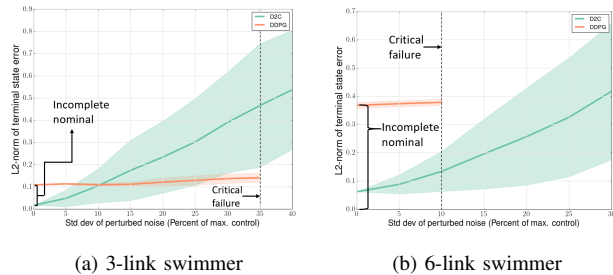


Fig. 3: D2C vs DDPG at $\Delta t = 0.01s$

decoupling based approaches such as D2C in a reinforcement learning paradigm and recognizes the need for more hybrid approaches that complement the merits of each other.

REFERENCES

- [1] P. R. Kumar and P. Varaiya, *Stochastic systems: Estimation, identification, and adaptive control*. SIAM, 2015, vol. 75.
- [2] P. A. Ioannou and J. Sun, *Robust adaptive control*. Courier Corporation, 2012.
- [3] K. J. Åström and B. Wittenmark, *Adaptive control*. Courier Corporation, 2013.
- [4] S. Sastry and M. Bodson, *Adaptive control: stability, convergence and robustness*. Courier Corporation, 2011.
- [5] D. Silver, A. Huang, C. J. Maddison, A. Guez, L. Sifre, G. Van Den Driessche, J. Schrittwieser, I. Antonoglou, V. Panneershelvam, M. Lanctot *et al.*, “Mastering the game of go with deep neural networks and tree search,” *nature*, vol. 529, no. 7587, p. 484, 2016.
- [6] T. P. Lillicrap, J. J. Hunt, A. Pritzel, N. Heess, T. Erez, Y. Tassa, D. Silver, and D. Wierstra, “Continuous control with deep reinforcement learning,” *arXiv preprint arXiv:1509.02971*, 2015.
- [7] S. Levine, C. Finn, T. Darrell, and P. Abbeel, “End-to-end training of deep visuomotor policies,” *The Journal of Machine Learning Research*, vol. 17, no. 1, pp. 1334–1373, 2016.
- [8] W. Yuhuai, M. Elman, L. Shun, G. Roger, and B. Jimmy, “Scalable

TABLE II: Simulation parameters and training outcomes

System	Steps per episode	Time-step (sec.)	Training time (sec.)		
			D2C		DDPG
			Open-loop	Closed-loop	
Inverted Pendulum	30	0.1	12.9	< 0.1	2261.15
Cart pole	30	0.1	15.0	1.33	6306.7
3-link Swimmer	1600	0.005	7861.0	13.1	38833.64
	800	0.01	4001.0	4.6	13280.7
6-link Swimmer	1500	0.006	9489.3	26.5	88160
	900	0.01	3585.4	16.4	15797.2
Fish	1200	0.005	6011.2	75.6	124367.6

trust-region method for deep reinforcement learning using kronecker-factored approximation,” *arXiv:1708.05144*, 2017.

- [9] S. John, L. Sergey, M. Philipp, J. Michael I., and A. Pieter, “Trust region policy optimization,” *arXiv:1502.05477*, 2017.
- [10] S. John, W. Filip, D. Prafulla, R. Alec, and K. Oleg, “Proximal policy optimization algorithms,” *arXiv:1707.06347*, 2017.
- [11] P. Henderson, R. Islam, P. Bachman, J. Pineau, D. Precup, and D. Meger, “Deep reinforcement learning that matters,” in *Thirty-Second AAAI Conference on Artificial Intelligence*, 2018.
- [12] S. Gu, T. Lillicrap, Z. Ghahramani, R. E. Turner, and S. Levine, “Q-prop: Sample-efficient policy gradient with an off-policy critic,” *arXiv preprint arXiv:1611.02247*, 2016.
- [13] M. Falcone, “Recent Results in the Approximation of Nonlinear Optimal Control Problems,” in *Large-Scale Scientific Computing LSSC*, 2013.
- [14] D. Jacobsen and D. Mayne, *Differential Dynamic Programming*. Elsevier, 1970.
- [15] E. Theodorou, Y. Tassa, and E. Todorov, “Stochastic Differential Dynamic Programming,” in *Proceedings of American Control Conference*, 2010.
- [16] E. Todorov and W. Li, “A generalized iterative LQG method for locally-optimal feedback control of constrained nonlinear stochastic systems,” in *Proceedings of American Control Conference*, 2005, pp. 300 – 306.
- [17] W. Li and E. Todorov, “Iterative linearization methods for approximately optimal control and estimation of non-linear stochastic system,” *International Journal of Control*, vol. 80, no. 9, pp. 1439–1453, 2007.
- [18] W. B. Powell, *Approximate Dynamic Programming: Solving the curses of dimensionality*. John Wiley & Sons, 2007.
- [19] D. Bertsekas, *Dynamic programming and optimal control*. Athena scientific Belmont, MA, 2012, vol. 2.
- [20] R. S. Sutton and A. G. Barto, *Reinforcement learning: An introduction*. MIT press, 2018.
- [21] W. H. Fleming, “Stochastic control for small noise intensities,” *SIAM J. Control*, vol. 9, no. 3, 1971.
- [22] A. E. Bryson and Y.-C. Ho, *Applied Optimal Control: Optimization, Estimation, and Control*. Routledge, New York, 1975.
- [23] T. Lillicrap *et al.*, “Continuous control with deep reinforcement learning,” in *Proc. ICLR*, 2016.
- [24] T. Emanuel, E. Tom, and Y. Tassa, “Mujoco: A physics engine for model-based control,” *IEEE/RSJ International Conference on Intelligent Robots and Systems*, pp. 5026–5033, 2012.
- [25] T. Yuval and *et al.*, “Deepmind control suite,” *arXiv:1801.00690*, 2018.
- [26] M. Plappert, “keras-rl,” <https://github.com/keras-rl/keras-rl>, 2016.
- [27] M. G. D. P. Riashat Islam, Peter Henderson, “Reproducibility of benchmarked deep reinforcement learning tasks for continuous control,” *Reproducibility in Machine Learning Workshop, ICML’17*, 2017.

In this supplementary document, there are two sections. Section I gives detailed proofs of the results outlined in the main manuscript. Section II gives additional empirical results to supplement those in the manuscript.

SUPPLEMENTARY MATERIAL I: PROOFS OF RESULTS

Proof of Lemma 1

Proof: We only consider the case when the state x_t is scalar, the vector case is straightforward to derive and only requires a more complex notation.

We proceed by induction. The first general instance of the recursion occurs at $t = 3$. It can be shown that:

$$\delta x_3 = \underbrace{(\bar{A}_2 \bar{A}_1(\epsilon w_0) + \bar{A}_2(\epsilon w_1) + \epsilon w_2)}_{\delta x_3^l} + \underbrace{\{\bar{A}_2 \bar{S}_1(\epsilon w_0) + \bar{S}_2(\bar{A}_1(\epsilon w_0) + \epsilon w_1 + \bar{S}_1(\epsilon w_0))\}}_{e_3}. \quad (19)$$

Noting that $\bar{S}_1(\cdot)$ and $\bar{S}_2(\cdot)$ are second and higher order terms, it follows that e_3 is $O(\epsilon^2)$.

Suppose now that $\delta x_t = \delta x_t^l + e_t$ where e_t is $O(\epsilon^2)$. Then:

$$\delta x_{t+1} = \bar{A}_{t+1}(\delta x_t^l + e_t) + \epsilon w_t + \bar{S}_{t+1}(\delta x_t), \\ = \underbrace{(\bar{A}_{t+1} \delta x_t^l + \epsilon w_t)}_{\delta x_{t+1}^l} + \underbrace{\{\bar{A}_{t+1} e_t + \bar{S}_{t+1}(\delta x_t)\}}_{e_{t+1}}. \quad (20)$$

Noting that \bar{S}_t is $O(\epsilon^2)$ and that e_t is $O(\epsilon^2)$ by assumption, the result follows that e_{t+1} is $O(\epsilon^2)$.

Now, let us take a closer look at the term e_t and again proceed by induction. It is clear that $e_1 = e_1^{(2)} = 0$. Next, it can be seen that $e_2 = \bar{A}_1 e_1^{(2)} + S_1^{(2)}(\delta x_1^l)^2 + O(\epsilon^3) = \bar{S}_1^{(2)}(\epsilon w_0)^2 + O(\epsilon^3)$, which shows the recursion is valid for $t = 2$ given it is so for $t = 1$.

Suppose that it is true for t . Then:

$$\delta x_{t+1} = \bar{A}_t \delta x_t + S_t(\delta x_t) + \epsilon w_t, \\ = \bar{A}_t(\delta x_t^l + e_t) + S_t(\delta x_t^l + e_t) + \epsilon w_t, \\ = \underbrace{(\bar{A}_t \delta x_t^l + \epsilon w_t)}_{\delta x_{t+1}^l} + \underbrace{\{\bar{A}_t e_t^{(2)} + S_t^{(2)}(\delta x_t^l)^2\}}_{e_{t+1}^{(2)}} + O(\epsilon^3), \quad (21)$$

where the last line follows because $e_t = e_t^{(2)} + O(\epsilon^3)$, and $\bar{S}_t(\cdot)$ contains second and higher order terms only. This completes the induction and the proof. ■

Proof of Lemma 2

Proof: We have that:

$$J^\pi = \sum_t \bar{c}_t + \sum_t \bar{C}_t(\delta x_t^l + e_t) + \sum_t \bar{H}_t(\delta x_t^l + e_t), \\ = \sum_t \bar{c}_t + \sum_t \bar{C}_t \delta x_t^l + \sum_t \delta x_t^l \bar{H}_t^{(2)} \delta x_t^l + \bar{C}_t e_t^{(2)} + O(\epsilon^3),$$

where the last line of the equation above follows from an application of Lemma 1. ■

Lemma 3

Lemma 3: Let $\delta J_1^\pi, \delta J_2^\pi$ be as defined in Lemma 2. Then, $\mathbb{E}[\delta J_1 \delta J_2] = 0$.

Proof: In the following, we suppress the explicit dependence on π for δJ_1^π and δJ_2^π for notational convenience. Recall that $\delta J_1 = \sum_{t=0}^T \bar{C}_t \delta x_t^l$, and $\delta J_2 = \sum_{t=0}^T \bar{H}_t(\delta x_t) + \bar{C}_t e_t$. For notational convenience, let us consider the scalar case, the vector case follows readily at the expense of more elaborate notation. We may write using Lemma 1:

$$\bar{H}_t(\delta x_t) + \bar{C}_t e_t = \bar{H}_t^{(2)}(\delta x_t^l)^2 + \bar{C}_t e_t^{(2)} + O(\epsilon^3), \\ = \sum_{\tau=0}^{t-1} q_{t,\tau}(\delta x_\tau^l)^2 + O(\epsilon^3), \quad (22)$$

for suitably defined coefficients $q_{t,\tau}$. Therefore, it follows that

$$\delta J_2 = \sum_{\tau=0}^T \bar{q}_{T,\tau}(\delta x_\tau^l)^2, \quad (23)$$

for suitably defined $\bar{q}_{T,\tau}$. Therefore:

$$\delta J_1 \delta J_2 = \sum_{t,\tau} \bar{C}_t(\delta x_t^l) \bar{q}_{T,t}(\delta x_t^l)^2. \quad (24)$$

Taking expectations on both sides:

$$E[\delta J_1 \delta J_2] = \sum_{t,\tau} \bar{C}_t \bar{q}_{T,t} E[\delta x_t^l(\delta x_t^l)^2]. \quad (25)$$

Break $\delta x_t^l = (\delta x_t^l - \delta x_\tau^l) + \delta x_\tau^l$, assuming $\tau < t$. Then, it follows that:

$$E[\delta x_\tau^l(\delta x_t^l)^2] = E[\delta x_\tau^l(\delta x_t^l - \delta x_\tau^l)^2] + E[(\delta x_\tau^l)^3] \\ + 2E[(\delta x_t^l - \delta x_\tau^l)(\delta x_\tau^l)^2] \\ = E[(\delta x_\tau^l)^3], \quad (26)$$

where the first and last terms in the first equality drop out due to the independence of the increment $(\delta x_t^l - \delta x_\tau^l)$ from δx_τ^l , and the fact that $E[\delta x_t^l - \delta x_\tau^l] = 0$ and $E[(\delta x_\tau^l)^3] = 0$. Since δx_τ^l is the state of the linear system $\delta x_{t+1} = \bar{A}_t \delta x_t^l + \epsilon w_t$, it may again be shown that:

$$E[(\delta x_\tau^l)^3] = \sum_{s_1, s_2, s_3} \Phi_{\tau, s_1} \Phi_{\tau, s_2} \Phi_{\tau, s_3} E[w_{s_1} w_{s_2} w_{s_3}], \quad (27)$$

where $\Phi_{t,\tau}$ represents the state transitions operator between times τ and t , and follows from the closed loop dynamics. Now, due to the independence of the noise terms w_t , it follows that $E[w_{s_1} w_{s_2} w_{s_3}] = 0$ regardless of s_1, s_2, s_3 .

An analogous argument as above can be repeated for the case when $\tau > t$. Therefore, it follows that $E[\delta J_1 \delta J_2] = 0$. ■

Proof of Proposition 1

Proof: It is useful to first write the sample path cost in a slightly different fashion. It can be seen that given sufficient smoothness of the requisite functions, the cost of any sample path can be expanded as follows:

$$J^\pi = \bar{J}^\pi + \epsilon J_1^\pi + \epsilon^2 J_2^\pi + \epsilon^3 J_3^\pi + \epsilon^4 J_4^\pi + \mathcal{R},$$

where:

$$\begin{aligned} J_1^\pi &= \mathcal{J}^1 \bar{\omega}, \\ J_2^\pi &= \bar{\omega}' \mathcal{J}^2 \bar{\omega}, \end{aligned}$$

and so on for J_3^π, J_4^π respectively, where \mathcal{J}^i are constant matrices (tensors) of suitable dimensions, and $\bar{\omega} = [\omega_1, \dots, \omega_N]$. Further, the remainder function \mathcal{R} is an $o(\epsilon^4)$ function in the sense that $\epsilon^{-4}\mathcal{R} \rightarrow 0$ as $\epsilon \rightarrow 0$.

Further, due to the whiteness of the noise sequences $\bar{\omega}$, it follows that $E[J_1^\pi] = 0$, and $E[J_3^\pi] = 0$, since these terms are made of odd valued products of the noise sequences, while $E[J_2^\pi], E[J_4^\pi]$ are both finite owing to the finiteness of the moments of the noise values and the initial condition. Further $\lim_{\epsilon \rightarrow 0} \epsilon^{-4} E[\mathcal{R}] = E[\lim_{\epsilon \rightarrow 0} \epsilon^{-4} \mathcal{R}] = 0$, i.e., $E[\mathcal{R}]$ is $o(\epsilon^4)$.

Therefore, using Lemma 2, and taking expectations on both sides, we obtain:

$$\begin{aligned} E[J^\pi] &= \bar{J}^\pi + E[\epsilon J_1^\pi] + E[\epsilon^2 J_2^\pi] + O(\epsilon^4) = \bar{J}^\pi + O(\epsilon^2), \\ \text{since } E[J_1^\pi] &= 0, \text{ and } E[\epsilon^2 J_2^\pi] \text{ is } O(\epsilon^2) \text{ due to the fact that } \\ E[J_2^\pi] &< \infty. \end{aligned}$$

Next, using Lemma 2, and taking the variances on both sides, and doing some work, we have:

$$\begin{aligned} \text{Var}[J^\pi] &= \text{Var}[\epsilon J_1^\pi] + E[\epsilon J_1^\pi \epsilon^2 J_2^\pi] + \text{Var}[\epsilon^2 J_2^\pi] + o(\epsilon^4) \\ &= \text{Var}[\delta J_1^\pi] + O(\epsilon^4), \end{aligned} \quad (28)$$

where the second equality follows from the fact that $E[\epsilon J_1^\pi \epsilon^2 J_2^\pi] = 0$ (proved in the appendix), and $\text{Var}[J_2^\pi] < \infty$. This completes the proof of the result. ■

Proof of Proposition 3

Proof: We have

$$\begin{aligned} \tilde{J}^{\pi^*} - \tilde{J}^{\pi^o} &= \tilde{J}^{\pi^*} - \bar{J}^{\pi^*} + \bar{J}^{\pi^*} - \tilde{J}^{\pi^o} \\ &\leq \tilde{J}^{\pi^*} - \bar{J}^{\pi^*} + \bar{J}^{\pi^o} - \tilde{J}^{\pi^o} \end{aligned}$$

The inequality above is due the fact that $\bar{J}^{\pi^*} \leq \bar{J}^{\pi^o}$, by definition of π^* . Now, using Proposition 1, we have that $|\tilde{J}^{\pi^*} - \bar{J}^{\pi^*}| = O(\epsilon^2)$, and $|\tilde{J}^{\pi^o} - \bar{J}^{\pi^o}| = O(\epsilon^2)$. Also, by definition, we have $\bar{J}^{\pi^o} \leq \tilde{J}^{\pi^*}$. Then, from the above inequality, we get

$$|\tilde{J}^{\pi^*} - \tilde{J}^{\pi^o}| \leq |\tilde{J}^{\pi^*} - \bar{J}^{\pi^*}| + |\bar{J}^{\pi^o} - \tilde{J}^{\pi^o}| = O(\epsilon^2)$$

A similar argument holds for the variance as well. ■

Proof of Proposition 4

In order to prove the result, we need some preliminaries. The dynamics are given by:

$$x_t = x_{t-1} + \bar{f}(x_{t-1})\Delta t + \bar{g}(x_{t-1})u_t\Delta t + \epsilon\omega_t\sqrt{\Delta t}, \quad (29)$$

where ω_t is a white noise sequence, and the sampling time Δt is small enough that $O(\Delta t^\alpha)$ is negligible for $\alpha > 1$. The noise term above is a Brownian motion, and hence the $\sqrt{\Delta t}$ factor. Further, the incremental cost function $c(x, u)$ is given as: $c(x, u) = \bar{l}(x)\Delta t + \frac{1}{2}u'Ru\Delta t$. The main reason to use the above assumptions is to simplify the Dynamic Programming

(DP) equation governing the optimal cost-to-go function of the system. The DP equation for the above system is given by:

$$J_t(x) = \min_{u_t} \{c(x, u) + E[J_{t+1}(x')]\}, \quad (30)$$

where $x' = x + \bar{f}(x)\Delta t + \bar{g}(x)u_t\Delta t + \epsilon\omega_t\sqrt{\Delta t}$. The above equation is marched back in time with terminal condition $J_T(x) = c_T(x)$, and $c_T(\cdot)$ is the terminal cost function. Then, it follows that the optimal control u_t satisfies (since the argument to be minimized is quadratic in u_t)

$$u_t = -R^{-1}\bar{g}'J_{t+1}^x, \quad (31)$$

where $J_{t+1}^x = \frac{\partial J_{t+1}}{\partial x}$.

Further, let $u_t^d(\cdot)$ be the optimal control policy for the deterministic system, i.e., the system with $\epsilon = 0$. The optimal cost-to-go of the deterministic system, $\phi_t(\cdot)$ satisfies the deterministic DP equation:

$$\phi_t(x) = \min_u [c(x, u) + \phi_{t+1}(x')], \quad (32)$$

where $x' = x + \bar{f}(x')\Delta t + \bar{g}(x')u\Delta t$. Then, identical to the stochastic case, $u_t^d = R^{-1}\bar{g}'\phi_t^x$. Next, let $\varphi_t(\cdot)$ denote the cost-to-go of the deterministic policy when applied to the stochastic system. The cost-to-go $\varphi_t(\cdot)$ satisfies the policy evaluation equation:

$$\varphi_t(x) = c(x, u_t^d(x)) + E[\varphi_{t+1}(x')], \quad (33)$$

where now $x' = x + \bar{f}(x)\Delta t + \bar{g}(x)u_t^d(x)\Delta t + \epsilon\omega_t\sqrt{\Delta t}$. Note the difference between the equations 32 and 33, and that $\phi_t \neq \varphi_t$.

Armed with the above developments, we are now ready to prove Proposition 4. In the following, we consider the case of a scalar state for convenience, the result is reasonably straightforward to generalize to the multivariable case. *Proof:* Using Proposition 1, we know that any cost function, and hence, the optimal cost-to-go function can be expanded as:

$$J_t(x) = J_t^0 + \epsilon^2 J_t^1 + \epsilon^4 J_t^2 + \dots \quad (34)$$

Thus, substituting the minimizing control in Eq. 31 into the dynamic programming Eq. 30 implies:

$$\begin{aligned} J_t(x) &= \bar{l}(x)\Delta t + \frac{1}{2}r\left(\frac{-\bar{g}}{r}\right)^2 (J_{t+1}^x)^2 \Delta t + J_{t+1}^x \bar{f}(x)\Delta t \\ &\quad + \bar{g}\left(\frac{-\bar{g}}{r}\right) (J_{t+1}^x)^2 \Delta t + \frac{\epsilon^2}{2} J_{t+1}^{xx} \Delta t + J_{t+1}(x), \end{aligned} \quad (35)$$

where J_t^x , and J_t^{xx} denote the first and second derivatives of the cost-to go function. Substituting Eq. 34 into eq. 35 we obtain that:

$$\begin{aligned} (J_t^0 + \epsilon^2 J_t^1 + \epsilon^4 J_t^2 + \dots) &= \bar{l}(x)\Delta t + \\ &\quad \frac{1}{2} \frac{\bar{g}^2}{r} (J_{t+1}^{0,x} + \epsilon^2 J_{t+1}^{1,x} + \dots)^2 \Delta t \\ &\quad + (J_{t+1}^{0,x} + \epsilon^2 J_{t+1}^{1,x} + \dots) \bar{f}(x)\Delta t \\ &\quad - \frac{\bar{g}^2}{r} (J_{t+1}^{0,x} + \epsilon^2 J_{t+1}^{1,x} + \dots)^2 \Delta t \\ &\quad + \frac{\epsilon^2}{2} (J_{t+1}^{0,xx} + \epsilon^2 J_{t+1}^{1,xx} + \dots) \Delta t + J_{t+1}(x). \end{aligned} \quad (36)$$

Now, we equate the ϵ^0 , ϵ^2 terms on both sides to obtain perturbation equations for the cost functions $J_t^0, J_t^1, J_t^2 \dots$. First, let us consider the ϵ^0 term. Utilizing Eq. 36 above, we obtain:

$$J_t^0 = \bar{l}\Delta t + \frac{1}{2} \frac{\bar{g}^2}{r} (J_{t+1}^{0,x})^2 \Delta t + \underbrace{(\bar{f} + \bar{g} \frac{-\bar{g}}{r} J_t^{0,x})}_{\bar{f}^0} J_t^{0,x} \Delta t + J_{t+1}^0, \quad (37)$$

with the terminal condition $J_T^0 = c_T$, and where we have dropped the explicit reference to the argument of the functions x for convenience.

Similarly, one obtains by equating the $O(\epsilon^2)$ terms in Eq. 36 that:

$$J_t^1 = \frac{1}{2} \frac{\bar{g}^2}{r} (2J_{t+1}^{0,x} J_{t+1}^{1,x}) \Delta t + J_{t+1}^{1,x} \bar{f} \Delta t - \frac{\bar{g}^2}{r} (2J_{t+1}^{0,x} J_{t+1}^{1,x}) \Delta t + \frac{1}{2} J_{t+1}^{0,xx} \Delta t + J_{t+1}^1, \quad (38)$$

which after regrouping the terms yields:

$$J_t^1 = \underbrace{(\bar{f} + \bar{g} \frac{-\bar{g}}{r} J_{t+1}^{0,x})}_{=\bar{f}^0} J_{t+1}^{1,x} \Delta t + \frac{1}{2} J_{t+1}^{0,xx} \Delta t + J_{t+1}^1, \quad (39)$$

with terminal boundary condition $J_T^1 = 0$. Note the perturbation structure of Eqs. 37 and 39, J_t^0 can be solved without knowledge of J_t^1, J_t^2 etc, while J_t^1 requires knowledge only of J_t^0 , and so on. In other words, the equations can be solved sequentially rather than simultaneously.

Now, let us consider the deterministic policy $u_t^d(\cdot)$ that is a result of solving the deterministic DP equation:

$$\phi_t(x) = \min_u [c(x, u) + \phi_{t+1}(x')], \quad (40)$$

where $x' = x + \bar{f}\Delta t + \bar{g}u\Delta t$, i.e., the deterministic system obtained by setting $\epsilon = 0$ in Eq. 29, and ϕ_t represents the optimal cost-to-go of the deterministic system. Analogous to the stochastic case, $u_t^d = \frac{-\bar{g}}{r} \phi_t^x$. Next, let φ_t denote the cost-to-go of the deterministic policy $u_t^d(\cdot)$ when applied to the stochastic system, i.e., Eq. 29 with $\epsilon > 0$. Then, the cost-to-go of the deterministic policy, when applied to the stochastic system, satisfies:

$$\varphi_t = c(x, u_t^d(x)) + E[\varphi_{t+1}(x')], \quad (41)$$

where $x' = \bar{f}\Delta t + \bar{g}u_t^d\Delta t + \epsilon\sqrt{\Delta t}\omega_t$. Substituting $u_t^d(\cdot) = \frac{-\bar{g}}{r} \phi_t^x$ into the equation above implies that:

$$\begin{aligned} \varphi_t &= \varphi_t^0 + \epsilon^2 \varphi_t^1 + \epsilon^4 \varphi_t^2 + \dots \\ &= \bar{l}\Delta t + \frac{1}{2} \frac{\bar{g}^2}{r} (\phi_{t+1}^x)^2 \Delta t + (\varphi_{t+1}^{0,x} + \epsilon^2 \varphi_{t+1}^{1,x} + \dots) \bar{f} \Delta t \\ &\quad + \bar{g} \frac{-\bar{g}}{r} \phi_{t+1}^x (\varphi_{t+1}^{0,x} + \epsilon^2 \varphi_{t+1}^{1,x} + \dots) \Delta t \\ &\quad + \frac{\epsilon^2}{2} (\varphi_{t+1}^{0,xx} + \epsilon^2 \varphi_{t+1}^{1,xx} + \dots) \Delta t \\ &\quad + (\varphi_{t+1}^0 + \epsilon^2 \varphi_{t+1}^1 + \dots). \quad (42) \end{aligned}$$

As before, if we gather the terms for ϵ^0 , ϵ^2 etc. on both sides of the above equation, we shall get the equations governing φ_t^0, φ_t^1 etc. First, looking at the ϵ^0 term in Eq. 39, we obtain:

$$\varphi_t^0 = \bar{l}\Delta t + \frac{1}{2} \frac{\bar{g}^2}{r} (\phi_{t+1}^x)^2 \Delta t + (\bar{f} + \bar{g} \frac{-\bar{g}}{r} \phi_{t+1}^x) \varphi_{t+1}^{0,x} \Delta t + \varphi_{t+1}^0, \quad (43)$$

with the terminal boundary condition $\varphi_T^0 = c_T$. However, the deterministic cost-to-go function also satisfies:

$$\phi_t = \bar{l}\Delta t + \frac{1}{2} \frac{\bar{g}^2}{r} (\phi_{t+1}^x)^2 \Delta t + (\bar{f} + \bar{g} \frac{-\bar{g}}{r} \phi_{t+1}^x) \phi_{t+1}^x \Delta t + \phi_{t+1}, \quad (44)$$

with terminal boundary condition $\phi_T = c_T$. Comparing Eqs. 43 and 44, it follows that $\phi_t = \varphi_t^0$ for all t . Further, comparing them to Eq. 37, it follows that $\varphi_t^0 = J_t^0$, for all t . Also, note that the closed loop system above, $\bar{f} + \bar{g} \frac{-\bar{g}}{r} \phi_{t+1}^x = \bar{f}^0$ (see Eq. 37 and 39).

Next let us consider the ϵ^2 terms in Eq. 42. We obtain:

$$\begin{aligned} \varphi_t^1 &= \bar{f} \varphi_{t+1}^{1,x} \Delta t + \bar{g} \frac{-\bar{g}}{r} \phi_{t+1}^x \varphi_{t+1}^{1,x} \Delta t + \\ &\quad \frac{1}{2} \varphi_{t+1}^{0,xx} + \varphi_{t+1}^1. \quad (45) \end{aligned}$$

Noting that $\phi_t = \varphi_t^0$, implies that (after collecting terms):

$$\varphi_t^1 = \bar{f}^0 \varphi_{t+1}^{1,x} \Delta t + \frac{1}{2} \varphi_{t+1}^{0,xx} \Delta t + \varphi_{t+1}^1, \quad (46)$$

with terminal boundary condition $\varphi_N^1 = 0$. Again, comparing Eq. 46 to Eq. 39, and noting that $\varphi_t^0 = J_t^0$, it follows that $\varphi_t^1 = J_t^1$, for all t . This completes the proof of the result. ■

Proof of Proposition 6

Consider the Dynamic Programming equation for the deterministic cost-to-go function:

$$\phi_t(x_t) = \min_{u_t} Q_t(x_t, u_t) = \min_{u_t} \{c_t(x_t, u_t) + \phi_{t+1}(x_{t+1})\}$$

By Taylor's expansion about the nominal state at time $t + 1$,

$$\begin{aligned} \phi_{t+1}(x_{t+1}) &= \phi_{t+1}(\bar{x}_{t+1}) + G_{t+1} \delta x_{t+1} \\ &\quad + \frac{1}{2} \delta x_{t+1}' P_{t+1} \delta x_{t+1} + q_{t+1}(\delta x_{t+1}). \end{aligned}$$

Substituting the linearization of the dynamics, $\delta x_{t+1} = A_t \delta x_t + B_t \delta u_t + r_t(\delta x_t, \delta u_t)$ in the above expansion,

$$\begin{aligned} \phi_{t+1}(x_{t+1}) &= \phi_{t+1}(\bar{x}_{t+1}) + G_{t+1} (A_t \delta x_t + B_t \delta u_t + r_t(\delta x_t, \delta u_t)) \\ &\quad + (A_t \delta x_t + B_t \delta u_t + r_t(\delta x_t, \delta u_t))' P_{t+1} (A_t \delta x_t \\ &\quad + B_t \delta u_t + r_t(\delta x_t, \delta u_t)) + q_{t+1}(\delta x_{t+1}). \end{aligned}$$

Similarly, expand the incremental cost at time t about the nominal state,

$$\begin{aligned} c_t(x_t, u_t) &= \bar{l}_t + L_t \delta x_t + \frac{1}{2} \delta x_t' L_{tt} \delta x_t + \frac{1}{2} \delta u_t' R_t \bar{u}_t \\ &\quad + \frac{1}{2} \bar{u}_t' R_t \delta u_t + \frac{1}{2} \delta u_t' R_t \delta u_t + \frac{1}{2} \bar{u}_t' R_t \bar{u}_t + s_t(\delta x_t). \end{aligned}$$

$$\begin{aligned}
Q_t(x_t, u_t) &= \overbrace{[\bar{l}_t + \frac{1}{2}\bar{u}_t^\top R_t \bar{u}_t + \phi_{t+1}(\bar{x}_{t+1})]}^{\bar{\phi}_t(\bar{x}_t, \bar{u}_t)} \\
&+ \delta u_t' (B_t' \frac{P_{t+1}}{2} B_t + \frac{1}{2} R_t) \delta u_t + \delta u_t' (B_t' \frac{P_{t+1}}{2} A_t \delta x_t \\
&+ \frac{1}{2} R_t \bar{u}_t + B_t' \frac{P_{t+1}}{2} r_t) + (\delta x_t' A_t' \frac{P_{t+1}}{2} B_t + \frac{1}{2} \bar{u}_t R_t \\
&+ r_t' \frac{P_{t+1}}{2} B_t + G_{t+1} B_t) \delta u_t + \delta x_t' A_t' \frac{P_{t+1}}{2} A_t \delta x_t \\
&+ \delta x_t' \frac{P_{t+1}}{2} A_t' r_t + (r_t' \frac{P_{t+1}}{2} A_t + G_{t+1} A_t) \delta x_t \\
&+ r_t' \frac{P_{t+1}}{2} r_t + G_{t+1} r_t + q_t \equiv \bar{\phi}_t(\bar{x}_t, \bar{u}_t) + H_t(\delta x_t, \delta u_t).
\end{aligned}$$

Now, $\min_{u_t} Q_t(x_t, u_t) = \min_{\bar{u}_t} \bar{\phi}_t(\bar{x}_t, \bar{u}_t) + \min_{\delta u_t} H_t(\delta x_t, \delta u_t)$

First order optimality: Along the optimal nominal control sequence \bar{u}_t , it follows from the minimum principle that

$$\begin{aligned}
\frac{\partial c_t(x_t, u_t)}{\partial u_t} + \frac{\partial g(x_t)}{\partial u_t} \frac{\partial \phi_{t+1}(x_{t+1})}{\partial x_{t+1}} &= 0 \\
\Rightarrow R_t \bar{u}_t + B_t' G_{t+1}' &= 0 \tag{47}
\end{aligned}$$

By setting $\frac{\partial H_t(\delta x_t, \delta u_t)}{\partial \delta u_t} = 0$, we get:

$$\begin{aligned}
\delta u_t^* &= -S_t^{-1} (R_t \bar{u}_t + B_t' G_{t+1}') - S_t^{-1} (B_t' P_{t+1} A_t + \\
&(G_t \otimes \tilde{R}_{t,xu})') \delta x_t - S_t^{-1} (B_t' P_{t+1} r_t) \\
&= -S_t^{-1} (B_t' P_{t+1} A_t + \underbrace{(G_{t+1} \otimes \tilde{R}_{t,xu})'}_{K_t}) \delta x_t \\
&\quad + \underbrace{S_t^{-1} (-B_t' P_{t+1} r_t)}_{p_t}
\end{aligned}$$

where, $S_t = R_t + B_t' P_{t+1} B_t$.

$$\Rightarrow \delta u_t = K_t \delta x_t + p_t.$$

Substituting it in the expansion of J_t and regrouping the terms based on the order of δx_t (till 2^{nd} order), we obtain:

$$\begin{aligned}
\phi_t(x_t) &= \bar{\phi}_t(\bar{x}_t) + (L_t + (R_t \bar{u}_t + B_t' G_{t+1}') K_t + G_{t+1} A_t) \delta x_t \\
&+ \frac{1}{2} \delta x_t' (L_{tt} + A_t' P_{t+1} A_t - K_t' S_t K_t + G_{t+1} \otimes \tilde{R}_{t,xx}) \delta x_t.
\end{aligned}$$

Expanding the LHS about the optimal nominal state result in the recursive equations in Proposition 6.

SUPPLEMENTARY MATERIAL II: EMPIRICAL RESULTS

In this section, we provide missing details from the empirical results in the paper as well as additional experiments that we did for this work. The outline is as follows: in the first section, we give details for the MUJOCO models used in the paper, in the second section, we give details and additional results for the training tasks, while in the third section, we give empirical results for the effect of stochasticity in the dynamics on training. We close with a section on the implementational details of the DDPG algorithm used in this paper.

Model Details

In this subsection, we provide details of the MuJoCo models used in our simulations.

Inverted pendulum A swing-up task of this 2D system from its downright initial position is considered.

Cart-pole The state of a 4D under-actuated cart-pole comprises the angle of the pole, cart's horizontal position and their rates. Within a given horizon, the task is to swing-up the pole and balance it at the middle of the rail by applying a horizontal force on the cart.

3-link Swimmer The 3-link swimmer model has 5 degrees of freedom and together with their rates, the system is described by 10 state variables. The task is to solve the planning and control problem from a given initial state to the goal position located at the center of the ball. Controls can only be applied in the form of torques to two joints. Hence, it is under-actuated by 3 DOF.

6-link Swimmer The task with a 6-link swimmer model is similar to that defined in the 3-link case. However, with 6 links, it has 8 degrees of freedom and hence, 16 state variables, controlled by 5 joint motors.

Fish The fish model moves in 3D space, the torso is a rigid body with 6 DOF. The system is described by 26 dimensions of states and 6 control channels. Controls are applied in the form of torques to the joints that connect the fins and tails with the torso. The rotation of the torso is described using quaternions.

Training Comparison: Additional Results

3-link Swimmer. The training data and performance plots for the 3-link swimmer are shown in Fig.4.

Data Efficiency, Time Efficiency and Parameter Size. In Fig. 10, we give results of training D2C and DDPG with respect to the number of rollouts. This is in addition to the time plot given in Fig. 1. Note that the time efficiency of D2C is much better than DDPG while the data efficiency of DDPG seems better in that it needs fewer rollouts for convergence (albeit it does not converge to a successful policy for the fish, in the time allowed for training). In our opinion, the wide time difference is due to the disparity in the size of the feedback parametrization between the two methods. Table I summarizes the parameter size during the training of D2C and DDPG. The number of parameters optimized during D2C training is the number of actuators times the number of timesteps while the DDPG parameter size equals the size of the neural networks, which is much larger. Due to the much larger network size, the computation done per rollout is much higher for DDPG. We also note that the D2C uses a rather conservative and simplistic gradient descent technique for the open-loop search, and thus the open-loop code optimization can lead to much better data efficiency on part of D2C. Nonetheless, this can only result in a higher time efficiency on part of D2C. This is not surprising as the D2C primarily derives its efficiency from its compact parametrization of the feedback law.

Effect of D2C System Identification. As the design of the feedback controller depends on the result of the sys-

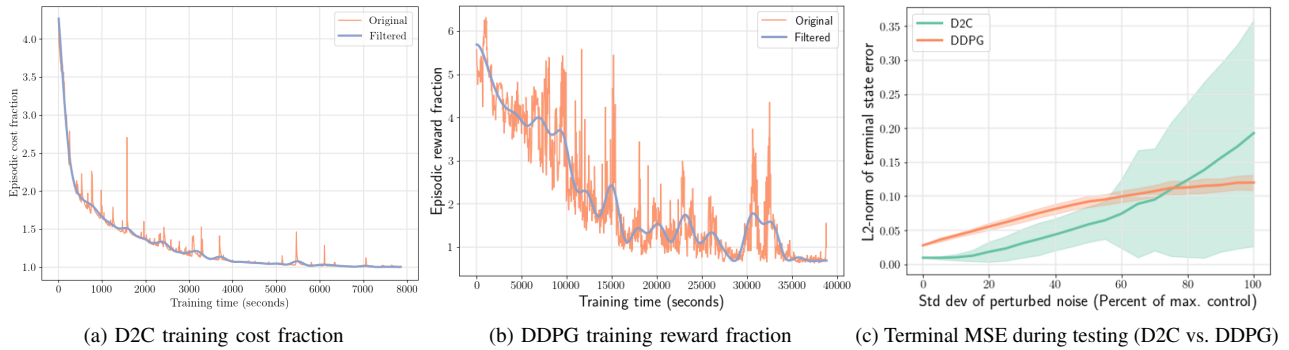


Fig. 4: Plots for 3-link swimmer

tem identification, the accuracy of the identified system is important for the closed-loop performance of D2C. Instead of the forward difference method reported in the main paper, we added a central-difference method to improve the identification accuracy. Figure. 5 shows the closed-loop performance plot for the 6-link swimmer example. Here the D2C feedback controller was designed based on the improved system identification result. Compared with Fig. 2(c), the D2C state error has lower mean and variance. With this improved result, it can be noted that D2C has comparable/better performance than DDPG until the noise level reaches about 50 percent.

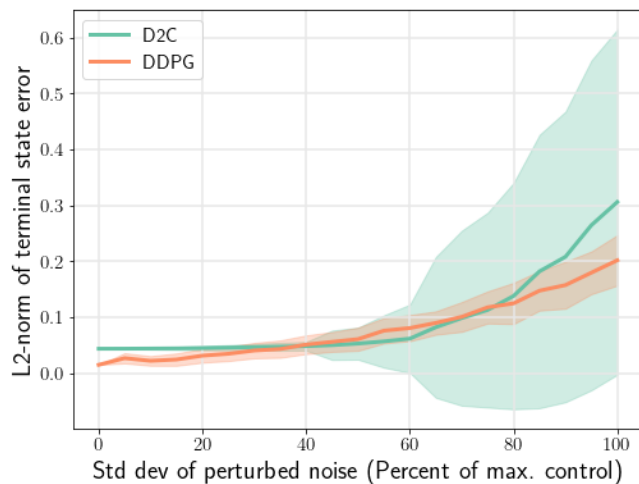


Fig. 5: Terminal MSE during testing(D2C vs. DDPG)

Reproducibility of Results. Reproducibility is still a major challenge that the field of reinforcement learning (RL) is yet to overcome. Despite significant progress in recent times, the difficulty in reproducing the results of the existing work made the reports of improvements over state-of-the-art RL methods questionable. Thus, we test the reproducibility of D2C by conducting multiple training sessions with the same hyperparameters but different random seeds. Figure. 8 shows the mean and the standard deviation of the episodic cost data

during training run 16 times each. For the inverted pendulum model and the cart-pole model, the results of all the training experiments are almost the same. Even for more complex models like the 6-link swimmer and the fish, the training is stable and the variance is small. Figure. 9 compares D2C with DDPG in the 3-link swimmer environment. Both algorithms run 4 repeated training experiments. It is evident that the variation of D2C is small and stable throughout the training whereas DDPG has a large variance even after it seems to be converged (note that the variable on the y-axis is not the absolute cost, but is scaled w.r.t. averaged cost during testing). After they both converge, the variation of D2C is still smaller than DDPG. It is evident that given the set of hyperparameters, D2C always results in the same policy (with a very small variance) unlike the results of the baseline RL algorithms also reported in [27]. This shows that D2C is more reliable and stable in training, thus has an advantage in reproducibility. This is an important feature in parameter tuning as the effects of changed parameters can be clearly demonstrated which makes selecting the best parameter set more efficient. Finally, in the spirit of reproducibility, our hyperparameters are reported for each example in Table III.

TABLE III: D2C parameters

System	Std of noise	Stepsize	Cost parameters*		
			Q	Q_t	R
Inverted Pendulum	0.0005	0.00018	0	700	0
Cart pole	0.07	0.005	10	(200, 100, 500, 100)	0
3-link Swimmer	0.2	0.022	2.5	2000	0.001
6-link Swimmer	0.2	0.018	2	200	0.001
Fish	0.05	0.0004	0.3	260	0.1

* Q is the incremental cost matrix, Q_t is the terminal cost matrix and R is the control cost matrix, all of which are diagonal matrices. If the diagonal elements have the same value, only one of them is presented in the table, otherwise all diagonal values are presented.

Robustness to Noise of D2C. Figure. 7 compared the

episodic cost during testing between the open-loop policy applied alone and the closed-loop policy. In the first case, the nominal control solution from open-loop optimization is applied without the feedback control. So the perturbation drives the model off the nominal trajectory and increases the episodic cost as the noise level increases. When the D2C closed-loop policy is applied, the episodic cost is much smaller in both mean and variance through the entire range of noise level considered, which shows a great improvement compared to the open-loop policy and proves the robustness of D2C. Moreover, Table II shows that most of the training time of D2C is consumed in the open-loop training part. Therefore, in the implementation of D2C, the closed-loop part makes a great improvement in performance within a small time budget. Currently, in the open-loop part, a somewhat primitive first-order gradient descent method is used without tuning the parameters such as the rollout number per iteration to optimize the time taken. Thus, there is much potential to further improve the time-efficiency of D2C.

Effect of “Stochastic Dynamics” on Learning

A noteworthy facet of the D2C design is that it is agnostic to the uncertainty, encapsulated by ϵ , and the near-optimality stems from the goodness of the deterministic feedback law when applied to the stochastic system. One may then question the fact that the design is not for the true stochastic system, and thus, one may expect RL techniques to perform better since they are applicable to the stochastic system. However, in practice, most RL algorithms only consider the deterministic system, in the sense that the only noise in the training simulations is the exploration noise in the control, and not from a persistent process noise. We now show the effect of adding a persistent process noise with a small to moderate value of ϵ to the training of DDPG, in the control as well as the state.

We trained the DDPG policy on the pendulum, cart-pole and 3-link swimmer examples. To simulate the stochastic environment, Gaussian i.i.d. random noise is added to all the input channels as process noise. As usual, the noise level ϵ is the noise standard deviation divided by the maximum control value of the open-loop optimal control sequence. Figure. 6 shows the DDPG training curve under different levels of process noise. As the process noise increases, the episodic cost converges slower and to a worse policy. When the process noise is larger than a threshold, the algorithm may altogether fail to converge for a given time budget. The problem is greatly exacerbated in the presence of state noise as seen from Fig. 6 that results in non-convergence or bad policies in the different examples for even small levels of noise. Hence, although theoretically, RL algorithms such as DDPG can train on the stochastic system, in practice, the process noise level ϵ must be limited to a small value for training convergence and/or good policies. Thus, this begs the question as to whether we should train on the stochastic system rather than appeal to the decoupling result that the deterministic policy is $O(\epsilon^4)$ near-optimal to the optimal stochastic policy, and thus train on the deterministic system. In summary, we note that this is

preliminary data and one of our research goals is to explore this aspect of the RL problem in much greater detail. The key stumbling block in this endeavor is the generation of training data due to the very long training times and will require a significant amount of computing time investment on our side which could not be done as of the writing of this paper.

DDPG Algorithm Implementation Details

Deep Deterministic Policy Gradient (DDPG) is a policy-gradient based off-policy reinforcement learning algorithm that operates in continuous state and action spaces. It relies on two function approximation networks one each for the actor and the critic. The critic network estimates the $Q(s, a)$ value given the state and the action taken, while the actor network engenders a policy given the current state. Neural networks are employed to represent the networks.

The off-policy characteristic of the algorithm employs a separate behavioral policy by introducing additive noise to the policy output obtained from the actor network. The critic network minimizes loss based on the temporal-difference (TD) error and the actor network uses the deterministic policy gradient theorem to update its policy gradient as shown below:

Critic update by minimizing the loss:

$$L = \frac{1}{N} \sum_i (y_i - Q(s_i, a_i | \theta^Q))^2$$

Actor policy gradient update:

$$\nabla_{\theta^\mu} \approx \frac{1}{N} \sum_i \nabla_a Q(s, a | \theta^Q) |_{s=s_i, a=\mu(s_i)} \nabla_{\theta^\mu} \mu(s | \theta^\mu) |_{s_i}$$

The actor and the critic networks consist of two hidden layers with the first layer containing 400 (*relu* activated) units followed by the second layer containing 300 (*relu* activated) units. The output layer of the actor network has the number of (*tanh* activated) units equal to that of the number of actions in the action space.

Target networks one each for the actor and the critic are employed for a gradual update of network parameters, thereby reducing the oscillations and a better training stability. The target networks are updated at $\tau = 0.001$. Experience replay is another technique that improves the stability of training by training the network with a batch of randomized data samples from its experience. We have used a batch size of 32 for the inverted pendulum and the cart pole examples, whereas it is 64 for the rest. Finally, the networks are compiled using Adams’ optimizer with a learning rate of 0.001.

To account for state-space exploration, the behavioral policy consists of an off-policy term arising from a random process. We obtain discrete samples from the Ornstein-Uhlenbeck (OU) process to generate noise as followed in the original DDPG method. The OU process has mean-reverting property and produces temporally correlated noise samples as follows:

$$dx_t = \Theta(\mu - x_t)dt + \sigma dW$$

where Θ indicates how fast the process reverts to mean, μ is the equilibrium or the mean value and σ corresponds to the degree of volatility of the process. Θ is set to 0.15, μ to 0 and σ is annealed from 0.35 to 0.05 over the training process.

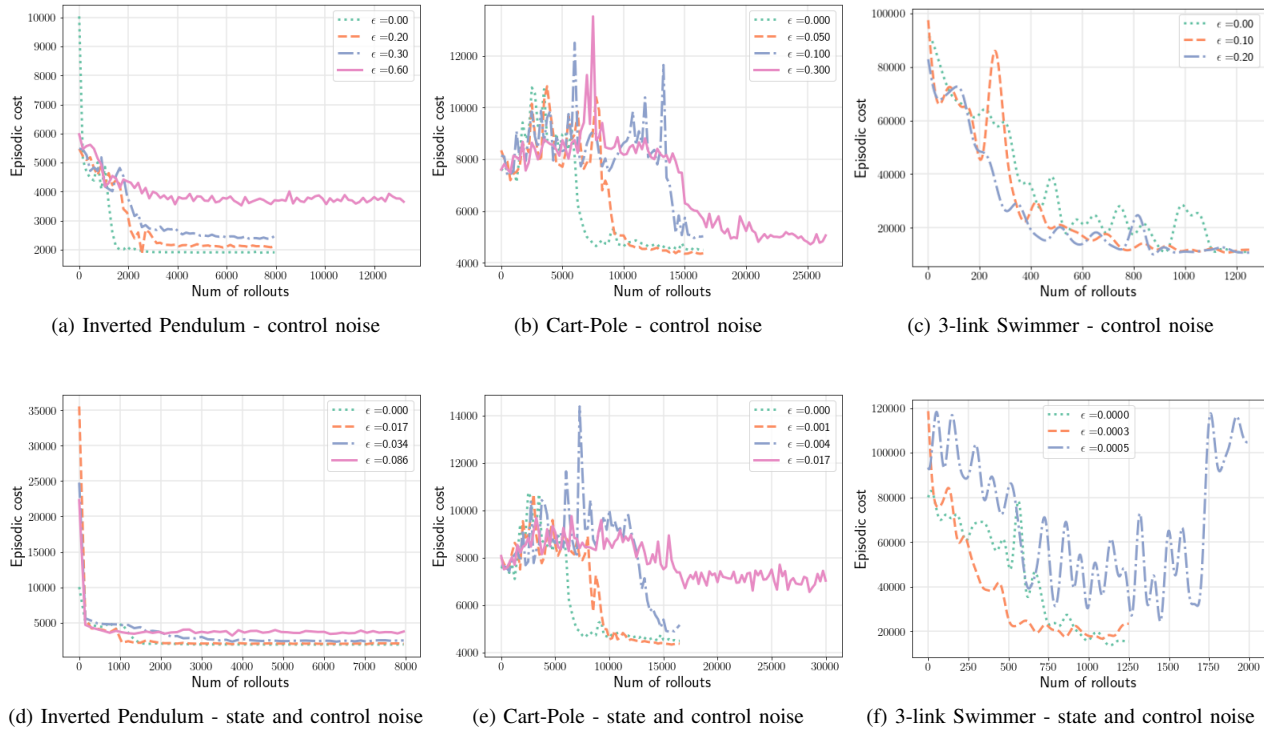


Fig. 6: Episodic cost vs number of rollouts taken during training with process noise for DDPG

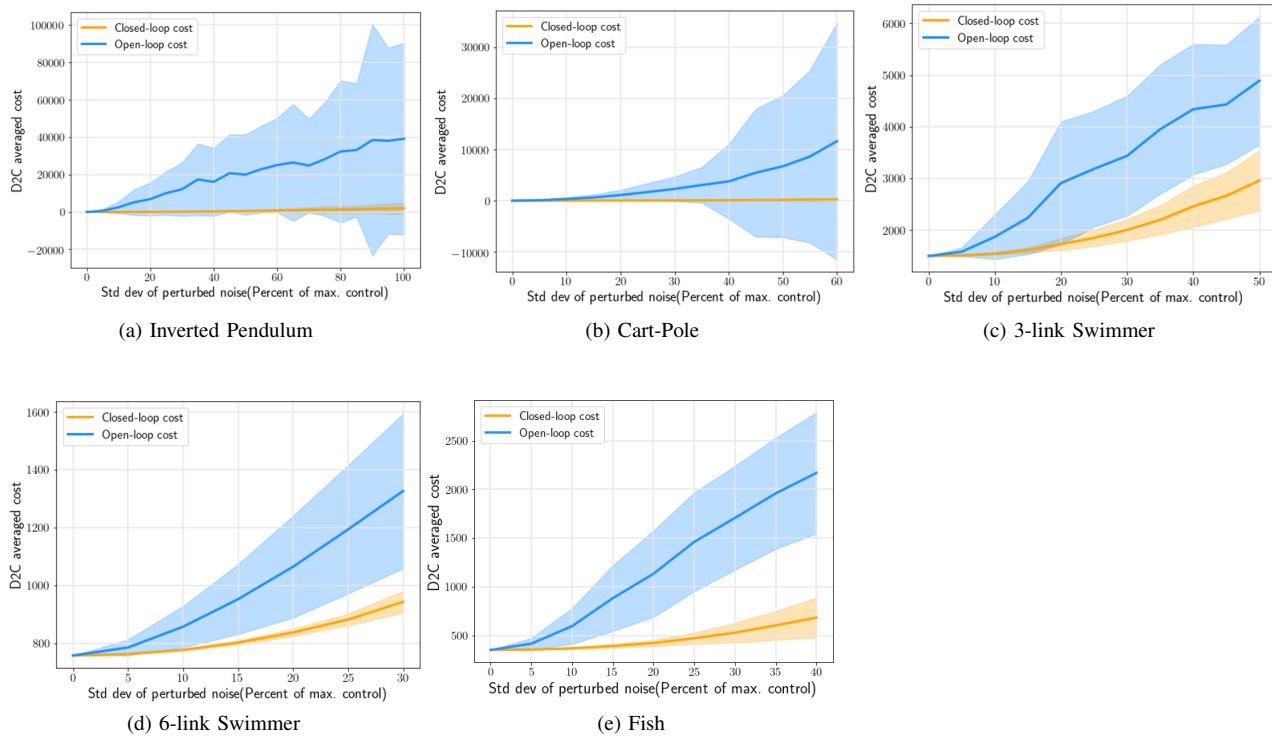
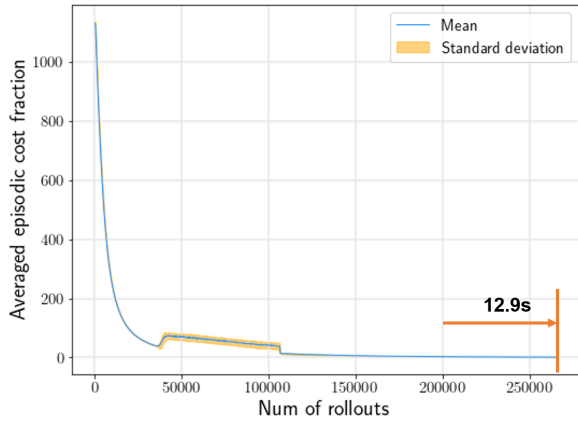
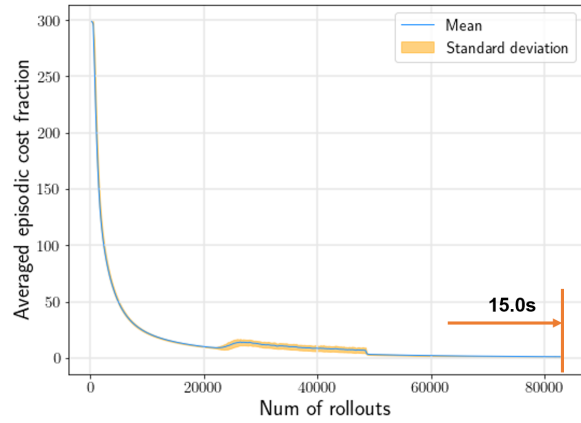


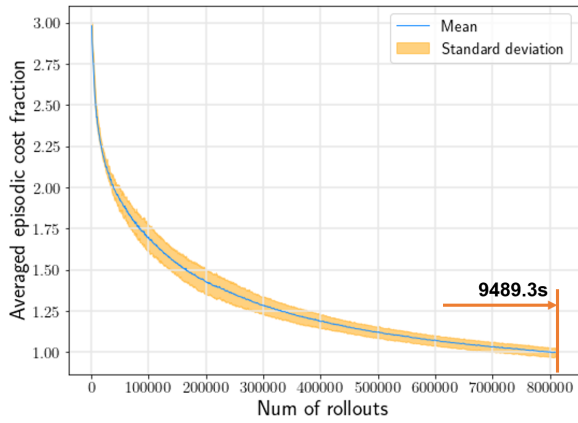
Fig. 7: Averaged episodic reward fraction vs noise level during testing for D2C



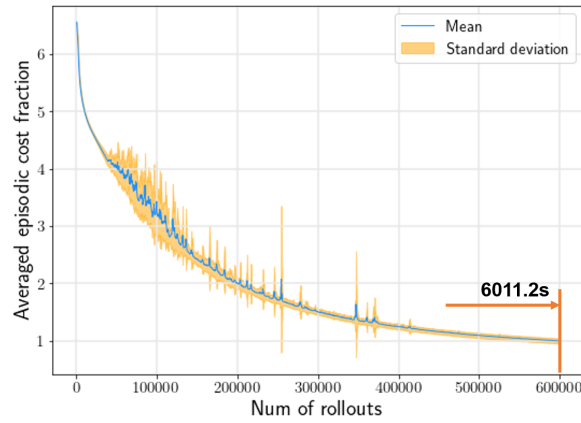
(a) Inverted Pendulum (DDPG)



(b) Cart-Pole

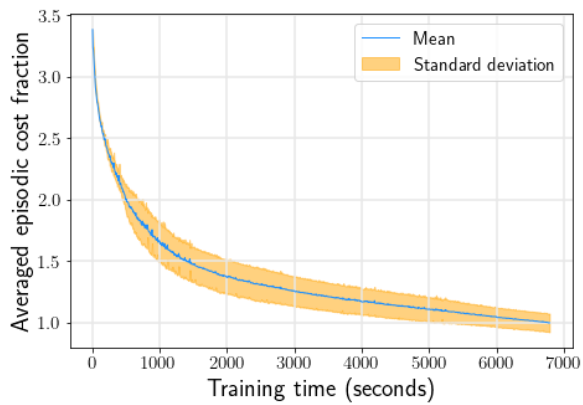


(c) 6-link Swimmer

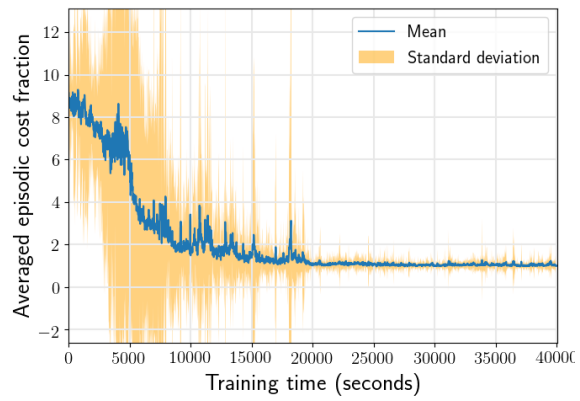


(d) Fish

Fig. 8: Averaged episodic cost fraction vs number of rollouts taken during training for D2C

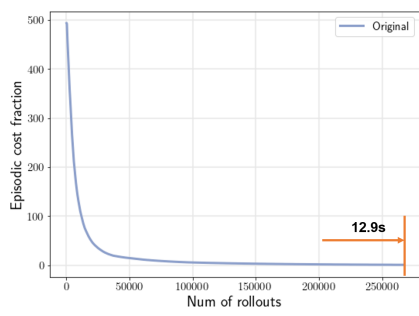


(a) 3-link Swimmer D2C

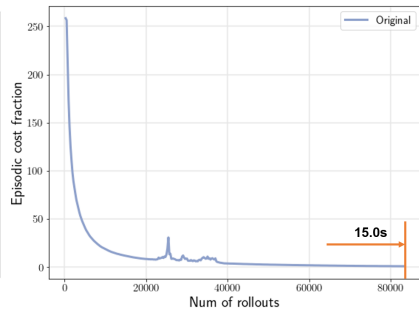


(b) 3-link Swimmer DDPG

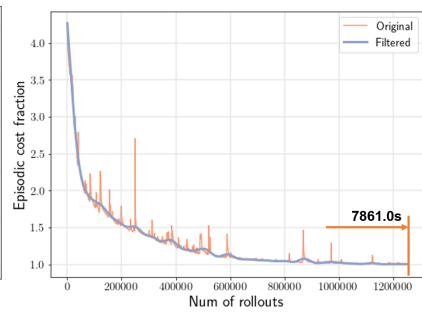
Fig. 9: Averaged episodic reward/cost fraction vs time taken during 4 training sessions



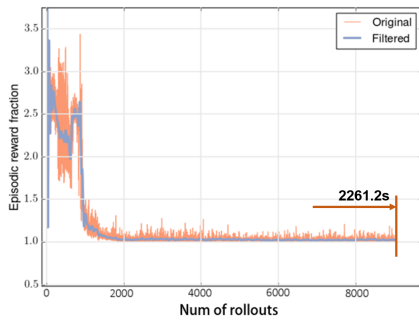
(a) Inverted Pendulum D2C



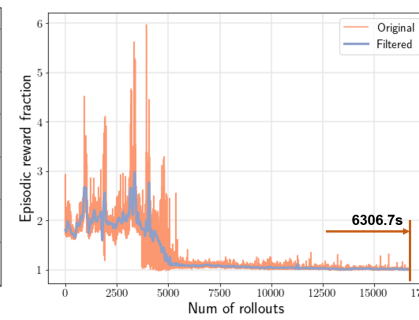
(b) Cart-Pole D2C



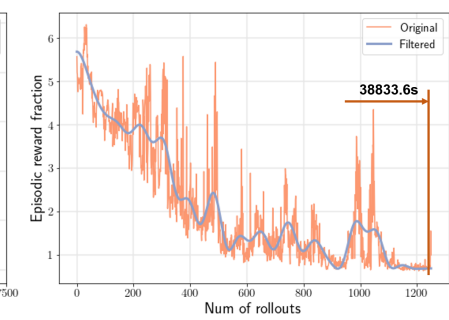
(c) 3-link Swimmer D2C



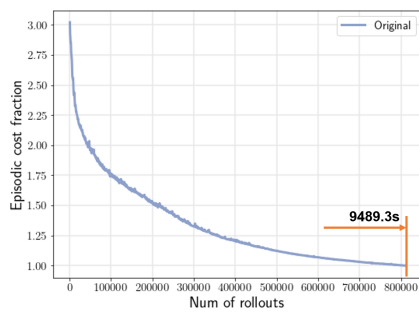
(d) Inverted Pendulum DDPG



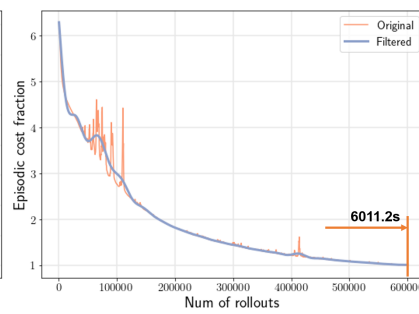
(e) Cart-Pole DDPG



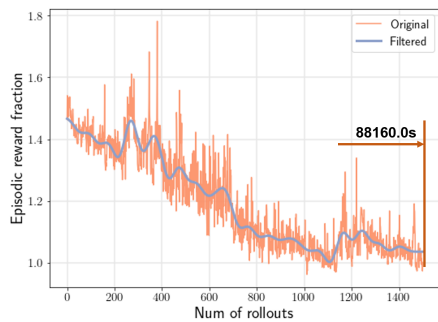
(f) 3-link Swimmer DDPG



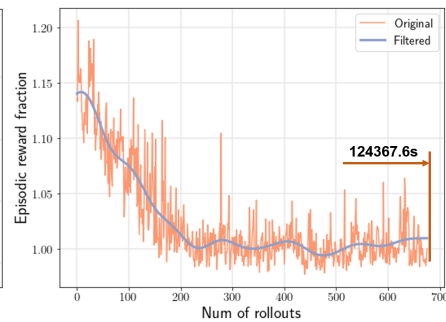
(g) 6-link Swimmer D2C



(h) Fish D2C



(i) 6-link Swimmer DDPG



(j) Fish DDPG

Fig. 10: Episodic reward/cost fraction vs number of rollouts taken during training